lek. dent. Paweł Sawicki

Wpływ parametrów ekspozycji badania tomografii komputerowej wiązki stożkowej na powstawanie artefaktów wokół wszczepów stomatologicznych.

Rozprawa na stopień doktora nauk medycznych i nauk o zdrowiu

w dyscyplinie nauki medyczne

Promotor: dr hab. n. med. Paweł J. Zawadzki

Promotor pomocniczy: dr n. med. Piotr Regulski

Klinika Chirurgii Czaszkowo-Szczękowo-Twarzowej, Chirurgii Jamy Ustnej i Implantologii,
Wydział Lekarsko-Stomatologiczny, Warszawski Uniwersytet Medyczny

Obrona rozprawy doktorskiej przed Radą Dyscypliny Nauk Medycznych

Warszawskiego Uniwersytetu Medycznego

Warszawa 2022 r.

Słowa kluczowe: tomografia komputerowa wiązki stożkowej, artefakty okołowszczepowe, wszczepy stomatologiczne, implantologia, ochrona radiologiczna

Keywords: cone beam computed tomography, peri-implant artifacts, dental implants, implantology, radiation protection

Wykaz publikacji stanowiących rozprawę doktorską:

1. **Sawicki P.,** Regulski P., Winiarski A., Zawadzki P. J., Influence of Exposure Parameters and Implant Position in Peri-Implant Bone Assessment in CBCT Images: An In Vitro Study. J. Clin. Med. 2022, 11,3846.
   https://doi.org/10.3390/jcm11133846
   (praca oryginalna)

   Lista MNiSW czasopism naukowych: 140 pkt
   Impact Factor: 4,964

2. **Sawicki P.**, Zawadzki P. J., Regulski P. (March 10, 2022), The Impact of Cone-Beam Computed Tomography Exposure Parameters on Peri-Implant Artifacts: A Literature Review. Cureus 14(3): e23035.
   https://doi.org/10.7759/cureus.23035
   (praca poglądowa)

   Lista MNiSW czasopism naukowych: 20 pkt

Sumaryczna liczba punktów MNiSW: 160 pkt
Sumaryczny Impact Factor: 4,964

Spis treści

I. Lista i objaśnienie stosowanych skrótów

CBCT – tomografia komputerowa wiązką stożkową (ang. cone beam computed tomography)

MSE – błąd średniokwadratowy (ang. mean squared error)

DICOM – obrazowanie cyfrowe i wymiana obrazów w medycynie (ang. Digital Imaging and Communications in Medicine)

II. Streszczenie w języku polskim:

Wstęp

Tomografia komputerowa wiązką stożkową (CBCT) jest popularną metodą oceny tkanki kostnej wokół wszczepów stomatologicznych. Mimo jej niepodważalnych zalet obecność metalowych struktur, jakimi są wszczepy stomatologiczne, indukuje powstawanie artefaktów zaburzających ocenę otaczających struktur. Celem cyklu publikacji jest ocena wpływu parametrów ekspozycji CBCT na powstawanie artefaktów wokół wszczepów stomatologicznych oraz możliwość oceny tkanki kostnej otaczającej implant.

Metodologia

Wykonano przegląd piśmiennictwa z użyciem elektronicznej bazy MEDLINE (PubMed) wyszukując publikacje opublikowane przed lipcem 2021 r. w języku angielskim, stosując zapytanie wyszukiwawcze „(dental OR dentistry) AND implant AND (artifact OR artifacts)". Przegląd piśmiennictwa uzupełniono o ręczne przeszukanie bazy danych. Na podstawie przeszukiwania bazy MEDLINE do oceny zakwalifikowano 378 publikacji. 46 publikacji włączono do przeglądu piśmiennictwa po wcześniejszym odrzuceniu prac na podstawie tytułu oraz ocenie prac pełnotekstowych oraz dodaniu prac z ręcznego przeszukiwania bazy publikacji.

10 tytanowych wszczepów stomatologicznych (InKone Primo, Global D, Paryż, Francja) wprowadzono w przygotowane wcześniej dwa modele kostne wykonane z fragmentów żeber wołowych. Wspomniane modele oraz model implantu połączonego z transferem wyciskowym zeskanowano za pomocą skanera laboratoryjnego 3shape E4 (3shape, Kopenhaga, Dania). Następnie dwa modele kostne poddano badaniu CBCT z zastosowaniem różnych parametrów napięcia (60, 70, 80, 90 kV), natężenia (4, 10 mA) oraz rozmiaru woksela (200, 300 µm). Przy pomocy oprogramowania do planowania implantologicznego BlueSkyPlan (BlueSkyBio, Libertyville, USA) nałożono na siebie obrazy badań radiologicznych oraz zeskanowanych modeli. Wykonano pomiary grubości przedsionkowej blaszki kostnej w dwóch wybranych okolicach zarówno w badaniach CBCT jak i przekrojach poprzecznych skanu modelu. Obliczono błąd średniokwadratowy (MSE - Mean Squared Error), będący podniesioną do kwadratu różnicą wykonanych pomiarów, w celu oceny dokładności aparatu CBCT. Uzyskane wyniki poddano analizie

statystycznej przeprowadzając jednokierunkową analizę wariancji (ANOVA), przyjmując za poziom istotności statystycznej $p \leq 0{,}05$.

Wyniki

W pracy przeglądowej, bazując na 46 publikacjach, podsumowano dotychczasową wiedzę na temat wpływu parametrów ekspozycji na występowanie artefaktów wokół wszczepów stomatologicznych.

Wyniki badań własnych wykazały istotne statystycznie różnice pomiędzy napięciem i MSE ($p = 0{,}044$), jak również pomiędzy pozycją implantu a MSE ($p = 0{,}005$). Zaburzenia pomiarowe okazały się zależne od grubości blaszki kostnej – im większa jest mierzona odległość, tym większy jest błąd. Nie uzyskano istotności statystycznej dla natężenia (test t-Studenta, $p = 0{,}956$) oraz rozmiaru woksela (test t-Studenta, $p = 0{,}055$).

Wnioski

Jak wynika z piśmiennictwa, napięcie i natężenie lampy rentgenowskiej oraz wielkość pola obrazowania mają wpływ na występowanie artefaktów wokół wszczepów stomatologicznych. Przeprowadzone badanie pokazuje, że istnieje możliwość dokładnych pomiarów przedsionkowej blaszki kostnej (MSE poniżej 0,25) przy zastosowaniu napięcia o wartościach 70, 80 i 90 kV. Zmniejszenie natężenia lampy rentgenowskiej oraz zwiększenie rozmiaru woksela pozwala ograniczyć dawkę promieniowania rentgenowskiego z zachowaniem możliwości diagnostyki przedsionkowej blaszki kostnej wokół wszczepów stomatologicznych.

III. Streszczenie w języku angielskim

Title: **Influence of cone beam computed tomography exposure parameters on peri-implant artifacts formation.**

Introduction

Cone Beam Computed Tomography (CBCT) is a popular method to assess bone tissue around dental implants. Despite its undeniable advantages, the presence of metal structures, such as dental implants, causes the formation of artifacts that prevent proper assessment of the surrounding structures.

The aim of this series of publications is to assess the impact of CBCT exposure parameters on the formation of peri-implant artifacts and the possibility of peri-implant bone tissue assessment.

Methods

A literature review was performed using MEDLINE electronic database (PubMed) to search for English-language papers published before July 2021, using the search query "(dental OR dentistry) AND implant AND (artifact OR artifacts)." The literature review was supplemented by a manual search of the database. The MEDLINE database search yielded 378 relevant publications. Finally, 46 papers were included in the literature review after title-based rejection, evaluation of full text papers and inclusion of publications from the manual search of the database.

A total of 10 titanium dental implants (InKone Primo, Global D, Paris, France) were placed into two previously prepared bovine ribs. Two bone models and an implant-with-transfer model were scanned with a 3Shape E4 laboratory scanner (3shape, Copenhagen, Denmark). CBCT scans of the two bone models were taken with different values of voltage (60, 70, 80, 90 kV), tube current (4, 10 mA) and voxel size (200, 300 µm). An implant planning software BlueSkyPlan (BlueSkyBio, Libertyville, USA) was used for model superimposition. Measurements of the buccal bone thickness were performed in two selected regions, using both CBCT and scan cross-sections of the model. The Mean Squared Error (MSE), defined as the squared differences between measurements, was used to assess the accuracy of the CBCT device. The obtained results were analysed statistically by performing one-way analysis of variance (ANOVA), with statistical significance set at $p \leq 0.05$.

Results

This review, which was based on 46 publications, summarised the current knowledge on the impact of exposure parameters on the occurrence of peri-implant artifacts. The original paper showed statistically significant differences between voltage and MSE ($p = 0.044$), as well as between implant position and MSE ($p = 0.005$). Measurement distortions depend on the thickness of the bone margin, and the higher the distance to measure, the higher the error. No statistical significance was found for current (Student's t-test, $p = 0.956$) or voxel size (Student's t-test, $p = 0.055$).

Conclusions

The literature review showed that the voltage and current of an X-ray tube as well as the size of the imaging field influence peri-implant artifact formation. The study showed that accurate measurements of buccal bone thickness (MSE below 0.25) can be achieved with voltage values of 70, 80, and 90 kV. Reduced X-ray tube current and an increased voxel size allow to reduce the dose of X-ray radiation while still being able to assess the peri-implant buccal bone.

IV. Wprowadzenie

Planowanie leczenia implantologicznego wymaga szczegółowego badania klinicznego i radiologicznego pacjenta w celu zaplanowania przewidywalnego leczenia. Badanie radiologiczne powinno umożliwiać ocenę jakości i ilości tkanki kostnej potrzebnej do wprowadzenia wszczepu stomatologicznego. Wyniki badań Monje i wsp. wskazują, że obecność przedsionkowej blaszki kostnej o grubości co najmniej 1,5 mm wokół wszczepu stomatologicznego jest kluczowym czynnikiem dla uzyskania korzystnego estetycznego i funkcjonalnego wyniku leczenia implantologicznego [1]. Zdjęcia pantomograficzne i zębowe są powszechnie stosowane w kontroli pozabiegowej ze względu na niską dawkę promieniowania oraz niski koszt wykonania badania. Mimo ich niepodważalnych zalet, te dwuwymiarowe badania są niewystarczające ze względu na brak możliwości oceny grubości wyrostka zębodołowego oraz nakładanie się sąsiadujących struktur. Badanie CBCT umożliwia trójwymiarową ocenę jakości i objętości tkanki kostnej, co ustanowiło je złotym standardem diagnostyki przedimplantacyjnej [2]. W nowoczesnych aparatach CBCT, odpowiednio ustawiając parametry ekspozycji dawka efektywna promieniowania rentgenowskiego jest relatywnie niewielka i może wynosić 70 μSv przy zastosowaniu pola obrazowania o wymiarach 8x8 cm lub 121 μSv dla pola obrazowania o wymiarach 15x15 cm [3].

W związku z obserwowaną utratą kości brzeżnej wokół implantu, która wynosi 0,24mm ± 0,62mm po pierwszym roku od obciążenia protetycznego, konieczne jest prowadzenie kontroli klinicznej i radiologicznej tkanek okołowszczepowych pacjentów po zakończonym leczeniu implantoprotetycznym. Rekomendacje sugerują badanie periodontologiczne z oceną głębokości sondowania, obecności krwawienia i/lub treści ropnej oraz ocenę zdjęć wewnątrzustnych [4-6]. Brak odpowiedniego monitorowania statusu klinicznego i radiologicznego może prowadzić do powstania zaawansowanego ubytku okołowszczepowej tkanki kostnej [7]. Pomimo zalet CBCT, autorzy przeglądu wskazują, że obecność artefaktów może maskować osseointegrację, płytkie defekty kostne oraz inne rodzaje przejaśnień, co utrudnia wczesną diagnozę ubytków tkanki kostnej. Artefakty są częścią obrazu radiologicznego, który nie reprezentuje żadnej struktury anatomicznej w obrębie ocenianych struktur i najczęściej są generowane przez obiekty pochłaniające promieniowanie rentgenowskie [2]. Mimo ich występowania, kilka badań rekomenduje stosowanie CBCT w ocenie tkanki kostnej wokół wszczepów stomatologicznych. Jednakże rekomendacje Jacobs i wsp. (2018) zalecają kontrolę radiologiczną przy użyciu zdjęć zębowych [2, 8-13]. Obecne zalecenia rekomendują dalsze prace nad rozwojem technik trójwymiarowego obrazowania, takich jak CBCT, co pozwoli na pomiary okołowszczepowej tkanki kostnej [2, 14]. Wczesna ocena ubytków okołowszczepowej tkanki kostnej pozwala na wdrożenie odpowiedniego leczenia, takiego jak oczyszczenie powierzchni implantu, augmentacja tkanek miękkich i twardych oraz ewentualne usunięcie wszczepu stomatologicznego [2, 12, 15].

Najczęściej występującym artefaktem w badaniach radiologicznych obszaru szczękowo-twarzowego są błędy pomiarowe. Są one obserwowane zarówno w badaniach pantomograficznych, zębowych, jak i badaniach CBCT, uznawanych za najbardziej dokładne badanie w radiologii stomatologicznej [16-19]. Powodem występowania błędów pomiarowych może być efekt utwardzenia wiązki, efekt częściowej objętości oraz algorytmy redukcji artefaktów [20]. Zniekształcenia wymiarowe są najbardziej powszechne wokół metalowych przedmiotów i intensywność ich występowania zależy od parametrów ekspozycji CBCT, takich jak napięcie i pole obrazowania. Istnieje możliwość ograniczenia występowania obu wymienionych wyżej artefaktów przez modyfikację parametrów ekspozycji tj. zwiększenie napięcia lampy rentgenowskiej i ograniczenie pola obrazowania, co jednocześnie zwiększa dawkę promieniowania rentgenowskiego. Zmniejszenie natężenia i rozmiaru woksela wpływa na ilość szumu w otrzymanym obrazie oraz dawkę promieniowania rentgenowskiego. Podsumowanie możliwości modyfikacji parametrów ekspozycji oraz ich wpływu na występowanie artefaktów, jakość obrazu oraz dawkę promieniowania jest zawarte w pracy poglądowej dołączonej do cyklu publikacji niniejszej rozprawy doktorskiej [21].

Cykl przedstawia wyniki jednej pracy oryginalnej oraz jedną pracę poglądową:

- The Impact of Cone-Beam Computed Tomography Exposure Parameters on Peri-Implant Artifacts: A Literature Review [21]
- Influence of Exposure Parameters and Implant Position in Peri-Implant Bone Assessment in CBCT Images: An In Vitro Study [22]

Publikacja „The Impact of Cone-Beam Computed Tomography Exposure Parameters on Peri-Implant Artifacts: A Literature Review” jest przeglądem literatury dotyczącym współczesnej wiedzy na temat występowania artefaktów wokół wszczepów stomatologicznych oraz wpływu modyfikacji parametrów ekspozycji na ich występowanie.

Celem pracy oryginalnej „Influence of Exposure Parameters and Implant Position in Peri-Implant Bone Assessment in CBCT Images: An In Vitro Study" była ocena wpływu zniekształceń wymiarowych i ich zmian występujących wraz z modyfikacją parametrów ekspozycji na pomiary okołowszczepowej blaszki kostnej.

V. Założenia i cel pracy

Głównym założeniem prac składających się na rozprawę doktorską było istnienie związku parametrów ekspozycji z występowaniem artefaktów wokół wszczepów stomatologicznych.

Cele pracy:

1. Podsumowanie dotychczasowych badań dotyczących wpływu modyfikacji parametrów ekspozycji na występowanie artefaktów wokół wszczepów stomatologicznych.
2. Ocena wpływu zaburzeń pomiarowych wynikających z występowania artefaktów wokół wszczepów stomatologicznych na pomiary okołowszczepowej blaszki kostnej.
3. Ocena zmiany dokładności pomiaru okołowszczepowej blaszki kostnej przy modyfikacji parametrów ekspozycji takich jak napięcie, natężenie oraz rozmiar woksela.
4. Określenie parametrów ekspozycji umożliwiających uzyskanie niskiego błędu pomiarowego przy ocenie zachowując możliwie niską dawkę promieniowania rentgenowskiego.

VI. Omówienie cyklu

Praca przeglądowa podsumowuje wyniki dotychczasowych badań dotyczących wpływu napięcia oraz natężenia lampy rentgenowskiej, rozmiaru woksela, wielkości pola obrazowania, zakresu obrotu lampy rentgenowskiej oraz algorytmów redukcji artefaktów na jakość obrazu oraz nasilenie występowania artefaktów wokół wszczepów stomatologicznych.

Celem pracy oryginalnej była ocena wpływu zniekształceń wymiarowych i ich zmian wraz z modyfikacją parametrów ekspozycji badania CBCT na pomiary okołowszczepowej tkanki kostnej. Wykonano dwa modele kostne z wołowego żebra oczyszczonego z tkanek miękkich, do których wprowadzono 5 tytanowych wszczepów stomatologicznych (InKone Primo, Global D, Paryż, Francja). Wszczepy umieszczono w modelu kostnym zachowując różne wartości grubości blaszki kostnej wynoszące od 0 do 1,2mm. Do powierzchni modeli kostnych przymocowano znaczniki radiologiczne, a metalowe elementy pokryto preparatem Scan Spray (Renfert, Niemcy). Dwa modele kostne oraz model implantu połączonego z transferem wyciskowym zostały zeskanowane przy pomocą skanera 3shape E4 (3shape, Dania). Badanie CBCT przygotowanych modeli kostnych wykonano przy użyciu urządzenia Vatech Pax-i 3D (Vatech, Hwaseong, Korea). Przeprowadzono 16 ekspozycji CBCT każdego wszczepionego implantu z poniższymi wartościami napięcia: 60, 70, 80, 90 kV, natężenia: 4, 10 mA oraz rozmiaru woksela: 200, 300 µm. W programie BlueSkyPlan (BlueSkyBio, Libertyville, USA) wykonano superimpozycję wyeksportowanych modeli cyfrowych z uzyskanymi z badań CBCT plikami DICOM. Wyłączono algorytmy redukcji artefaktów. W uzyskanych badaniach wykonano 160 przekrojów poprzecznych przechodzących przez oceniane implanty, które poddano analizie.

Grubość okołowszczepowej blaszki kostnej została zmierzona w programie BlueSkyPlan (BlueSkyBio, Libertyville, USA) przy użyciu cyfrowej linijki w płaszczyźnie horyzontalnej w dwóch miejscach: platformy implantu (L1) oraz 3,5 mm wierzchołkowo od szyjki implantu (L2). Pomiary grubości blaszki kostnej uzyskane z modeli cyfrowych ustalono jako pomiary referencyjne. Pomiary w badaniach CBCT wykonano na tym samym poziomie co pomiary referencyjne. Obliczono średni błąd kwadratowy (MSE) będący podniesioną do kwadratu różnicą wykonanych pomiarów w celu oceny dokładności aparatu CBCT. Wszystkie pomiary zostały wykonane dwukrotnie, z zachowaniem co najmniej 6-tygodniowego odstępu pomiędzy nimi, by upewnić się, że są powtarzalne oraz pierwszy pomiar nie ma wpływu na kolejny. Wykonano ocenę wiarygodności pomiarów za pomocą analizy współczynnika korelacji wewnątrzklasowej. Obliczono średnią z wykonanych pomiarów, którą użyto w dalszej analizie statystycznej.

Przeprowadzono jednokierunkową analizę wariancji (ANOVA) do oceny zależności pomiędzy napięciem i MSE oraz pozycją implantu i MSE. Przeprowadzono testy t-Studenta dla oceny zależności pomiędzy natężeniem, rozmiarem woksela oraz MSE. Analiza regresji liniowej została użyta w celu odnalezienia zależności pomiędzy grubością blaszki kostnej oraz MSE dla każdego użytego napięcia. Zgodnie z tym równaniem, wybrano zakres grubości kości dla każdego MSE, które było mniejsze niż 0,25 mm^2, co odpowiada błędowi pomiarowemu wynoszącemu mniej niż 0,5 mm.

VII. Podsumowanie i wnioski

Przeprowadzone badania potwierdzają tezę, w której błąd pomiarowy w pomiarach przedsionkowej blaszki kostnej wokół wszczepów stomatologicznych zależy od napięcia i pozycji implantu. MSE istotnie statystycznie zmniejsza się wraz ze wzrostem napięcia i wzrostem grubości blaszki kostnej. Nie stwierdzono statystycznie istotnych różnic dla natężenia i rozmiaru woksela.

Wnioski

1. Dostępne piśmiennictwo wskazuje na to, że odpowiednie ustawienie napięcia, natężenia, rozmiaru woksela, pola obrazowania, zakresu rotacji aparatu CBCT oraz mechanizmy redukcji artefaktów mają wpływ na ilość występujących artefaktów oraz jakość obrazu w badaniu CBCT.
2. Zaburzenia pomiarowe wynikające z występowania artefaktów wokół wszczepów stomatologicznych mają istotny wpływ na pomiary okołowszczepowej blaszki kostnej.
3. Wzrost napięcia lampy rentgenowskiej powoduje poprawę dokładności pomiaru okołowszczepowej blaszki kostnej; modyfikacja natężenia i rozmiaru woksela nie ma wpływu na dokładność pomiaru okołowszczepowej blaszki kostnej.
4. Grubość okołowszczepowej blaszki kostnej może być zmierzona z błędem wynoszącym 0,5 mm dla napięcia wynoszącego 70, 80 i 90 kV. Zmniejszenie natężenia oraz zwiększenie rozmiaru woksela ogranicza dawkę promieniowania rentgenowskiego nie mając wpływu na dokładność pomiaru okołowszczepowej blaszki kostnej.

1. Monje, A., et al., *The Critical Peri-implant Buccal Bone Wall Thickness Revisited: An Experimental Study in the Beagle Dog.* Int J Oral Maxillofac Implants, 2019. **34**(6): p. 1328–1336.
2. Jacobs, R., et al., *Cone beam computed tomography in implant dentistry: recommendations for clinical use.* BMC Oral Health, 2018. **18**(1): p. 88.
3. McGuigan, M.B., H.F. Duncan, and K. Horner, *An analysis of effective dose optimization and its impact on image quality and diagnostic efficacy relating to dental cone beam computed tomography (CBCT).* Swiss Dent J, 2018. **128**(4): p. 297-316.
4. Maier, F.M., *Initial Crestal Bone Loss After Implant Placement with Flapped or Flapless Surgery-A Prospective Cohort Study.* Int J Oral Maxillofac Implants, 2016. **31**(4): p. 876-83.
5. Berglundh, T., et al., *Peri-implant diseases and conditions: Consensus report of workgroup 4 of the 2017 World Workshop on the Classification of Periodontal and Peri-Implant Diseases and Conditions.* J Periodontol, 2018. **89 Suppl 1**: p. S313-s318.
6. Papapanou, P.N., et al., *Periodontitis: Consensus report of workgroup 2 of the 2017 World Workshop on the Classification of Periodontal and Peri-Implant Diseases and Conditions.* J Periodontol, 2018. **89 Suppl 1**: p. S173-s182.
7. Dreyer, H., et al., *Epidemiology and risk factors of peri-implantitis: A systematic review.* J Periodontal Res, 2018. **53**(5): p. 657-681.
8. Mark, R., et al., *Comparative Evaluation of Periodontal Osseous Defects Using Direct Digital Radiography and Cone-Beam Computed Tomography.* J Pharm Bioallied Sci, 2021. **13**(Suppl 1): p. S306-s311.
9. Ruetters, M., et al., *Ex vivo comparison of CBCT and digital periapical radiographs for the quantitative assessment of periodontal defects.* Clin Oral Investig, 2020. **24**(1): p. 377-384.
10. Palkovics, D., et al., *Digital three-dimensional visualization of intrabony periodontal defects for regenerative surgical treatment planning.* BMC Oral Health, 2020. **20**(1): p. 351.
11. Woelber, J.P., et al., *Accuracy and Usefulness of CBCT in Periodontology: A Systematic Review of the Literature.* Int J Periodontics Restorative Dent, 2018. **38**(2): p. 289-297.
12. Song, D., et al., *Diagnostic accuracy of CBCT versus intraoral imaging for assessment of peri-implant bone defects.* BMC Medical Imaging, 2021. **21**(1): p. 23.
13. Golubovic, V., et al., *Accuracy of cone-beam computed tomography to assess the configuration and extent of ligature-induced peri-implantitis defects. A pilot study.* Oral Maxillofac Surg, 2012. **16**(4): p. 349-54.
14. Jacobs, R., et al., *CBCT vs other imaging modalities to assess peri-implant bone and diagnose complications: a systematic review.* Eur J Oral Implantol, 2018. **11 Suppl 1**: p. 77-92.
15. Hussain, R.A., M. Miloro, and J.B. Cohen, *An Update on the Treatment of Periimplantitis.* Dent Clin North Am, 2021. **65**(1): p. 43-56.
16. Kayal, R., *Distortion of digital panoramic radiographs used for implant site assessment.* journal of orthodontic science, 2016. **5**(4): p. 117-120.
17. Suphangul, S., et al., *Dimension distortion of digital panoramic radiograph on posterior mandibular regions.* Mahidol Dental Journal, 2016. **36**: p. 279-286.
18. Greenstein, G., J.S. Cavallaro, Jr., and D.P. Tarnow, *Clinical pearls for surgical implant dentistry: Part I.* Dent Today, 2010. **29**(5): p. 124-7.
19. Coelho-Silva, F., et al., *Distortion or magnification? An in vitro cone-beam CT study of dimensional changes of objects with different compositions.* Dentomaxillofac Radiol, 2021. **50**(8): p. 20210063.
20. Schulze, R.K., D. Berndt, and B. d'Hoedt, *On cone-beam computed tomography artifacts induced by titanium implants.* Clin Oral Implants Res, 2010. **21**(1): p. 100-7.
21. Sawicki, P., P.J. Zawadzki, and P. Regulski, *The Impact of Cone-Beam Computed Tomography Exposure Parameters on Peri-Implant Artifacts: A Literature Review.* Cureus, 2022. **14**(3): p. e23035.

22. Sawicki, P., et al., *Influence of Exposure Parameters and Implant Position in Peri-Implant Bone Assessment in CBCT Images: An In Vitro Study.* J Clin Med, 2022. **11**(13).

VIII. Kopie opublikowanych prac

Journal of
Clinical Medicine

MDPI

Article

Influence of Exposure Parameters and Implant Position in Peri-Implant Bone Assessment in CBCT Images: An In Vitro Study

Paweł Sawicki [1], Piotr Regulski [2,*], Artur Winiarski [3] and Paweł J. Zawadzki [1]

[1] Department of Cranio-Maxillofacial Surgery, Oral Surgery and Implantology, Faculty of Dental Medicine, Medical University of Warsaw, 02-005 Warsaw, Poland; kontakt@pawelsawicki.pl (P.S.); kcst@wum.edu.pl (P.J.Z.)
[2] Department of Dental and Maxillofacial Radiology, Faculty of Dental Medicine, Medical University of Warsaw, 61 Zwirki i Wigury Street, 02-091 Warsaw, Poland
[3] Department of Dental Propaedeutics and Prophylaxis, Faculty of Dental Medicine, Medical University of Warsaw, 02-006 Warsaw, Poland; artur.winiarski@wum.edu.pl
* Correspondence: piotr.regulski@wum.edu.pl

Abstract: The aim of this study was to assess the impact of dimensional distortion and its changes with modification of exposure setting parameters on the measurements of peri-implant bone margin. Ten titanium dental implants (InKone Primo, Global D, Paris, France) were placed in two prepared bovine ribs. Two bone models and an implant-with-transfer model were scanned with 3shape E4 (3shape, Copenhagen, Denmark) laboratory scanner. Cone beam computed tomography (CBCT) images of two bone models were taken with different values of voltage (60, 70, 80, 90 kV), tube current (4, 10 mA) and voxel size (200, 300 μm). All the data were superimposed using planning software, and the measurements of buccal bone thickness in two selected regions were performed both using CBCT and scan cross-sections. The mean squared error (MSE) being the squared differences between measurements was used in the accuracy assessment of the CBCT device. A one-way ANOVA revealed significant differences between voltage and MSE ($p = 0.044$), as well as implant position and MSE ($p = 0.005$). The distortions of measurements depend on bone margin thickness, and the higher the distance to measure, the higher the error. Accurate measurements of buccal bone thickness (MSE below 0.25) were achieved with voltage values of 70, 80, and 90 kV.

Keywords: CBCT; dental implants; buccal bone; peri-implant artifacts; dentistry

Citation: Sawicki, P.; Regulski, P.; Winiarski, A.; Zawadzki, P.J. Influence of Exposure Parameters and Implant Position in Peri-Implant Bone Assessment in CBCT Images: An In Vitro Study. *J. Clin. Med.* **2022**, *11*, 3846. https://doi.org/10.3390/jcm11133846

Academic Editor: Daniele De Santis

Received: 11 May 2022
Accepted: 30 June 2022
Published: 2 July 2022

1. Introduction

A decrease in the horizontal and vertical dimensions of the alveolar ridge is observed one year after tooth extraction due to bone resorption, which may be exacerbated by inflammatory processes of endodontic or periodontal origin [1,2].

Bone remodelling following tooth extraction can be partially reduced by procedures, such as alveolar ridge preservation, aiming to maintain the bone volume required for implant-supported prosthetic restoration [3–5]. When planning such treatment, a minimum of 1.5 mm of buccal bone width surrounding the implant should be provided, which according to Monje et al. is a key factor for favourable long-term aesthetic and functional outcome in dental implant treatment [6].

Due to the observed crestal bone loss subsequent to implant insertion, which averages 0.24mm ± 0.62mm after one year, a follow-up is mandatory to monitor soft and hard peri-implant tissues. Consensus reports recommend periodontal examination and charting (the presence/absence of bleeding and suppuration on probing and probing depth), as well as taking standardized intraoral radiographs [7–9].

Intraoral (IO) and panoramic radiographs are most commonly used during follow-up due to their low radiation dose and cost-effectiveness. Despite the undeniable advantages of the aforementioned two-dimensional (2D) imaging modalities, they do not allow the assessment of the buccal bone, which is crucial for successful implant treatment. It is possible to evaluate the buccal bone level and its thickness by bone sounding using a periodontal probe, which is an invasive procedure, as well as ultrasonography and cone beam computed tomography (CBCT), which is a three-dimensional (3D), non-invasive imaging modality [10–12].

Several studies recommend the use of CBCT for early evaluation of periodontal bone defects. However, due to artifact formation around dental implants, few studies recommend CBCT for bone assessment around dental implants [12–17]. Contemporary recommendations for the clinical use of CBCT in implant dentistry developed by Jacobs et al. (2018) indicate that although intraoral radiographs are still considered to be the primary tool for postoperative implant monitoring, we should realize that we need to evaluate three-dimensional bone healing, including morphological, volumetric, and trabecular remodelling [18]. Current guidelines recommend further work on the development of 3D imaging techniques, such as CBCT, which will allow for accurate measurements of peri-implant bone tissue [18,19]. Screening for peri-implant defects at early stages would allow for adequate treatment, such as debridement of the implant surface, bone, and/or soft tissue augmentation procedures or even removal of the dental implant [12,18,20].

Dimensional distortion is a common artifact in dental–maxillofacial radiology. Its presence has been confirmed on both periapical and panoramic radiographs [21–23]. Surprisingly, dimensional changes were also observed in CBCT, which is considered one of the most accurate techniques in dental radiology [24]. These distortions may be related to beam hardening, partial volume effects, and metallic artifact reduction algorithms [25].

Shape distortions are most common with metal and high radiosensitivity materials and depend on CBCT exposure parameters, such as voltage and field of view. Reduction of both voltage and field-of-view diminishes the amount of beam hardening artifacts and, at the same time, increases the radiation dose. Modification of other exposure parameters, such as tube current or voxel size, affects the amount of noise and radiation dose [26]. Once an appropriate field-of-view has been set up in accordance with the ALARA radiation safety principle (As Low As Reasonably Achievable), it remains necessary to set the remaining exposure parameters [27]. There is a need to find the optimal voltage, tube current, and voxel size settings that allow for the smallest possible measurement error in peri-implant bone assessment while maintaining a low radiation dose.

Reliance on dimensional distortion in the assessment of peri-implant tissues in CBCT images may lead to misdiagnosis and clinically unjustified treatment, which may even result in the deterioration of peri-implant tissues (i.e., peri-implant soft tissue dehiscence and deterioration of aesthetics) [28].

Therefore, the aim of this study was to assess the impact of shape distortion on the measurements of the bone margin surrounding dental implants. The effect of voltage, current, and voxel size was taken into consideration. The null hypothesis was that there was no significant difference between measurement error and voltage, current, implant position, or voxel size.

2. Materials and Methods

Two blocks of bovine ribs, obtained from a local slaughterhouse, were prepared and denuded from soft tissues. Bone materials were classified as medium dense (D2–D3) based on the section of fresh bovine rib, drilling resistance during implant bed preparation, and primary implant stability. In D2 type of bone, there is thick dense to porous cortical bone on the crest and coarse trabecular bone within. In D3 type of bone, there is thin, porous cortical bone on the crest and fine trabecular bone within. The D2 bone type is most suitable for implant placement and postoperative healing [29,30]. Ten implant site osteotomies were performed according to the manufacturer's instructions with a final 3.4 mm drill. Five dental implants (InKone Primo ∅ = 3.5 mm L = 8.5 mm, Global D, France) were placed into each fresh bovine rib (10 implants in total). Dental titanium implants used in this study are designed with an internal 8-degree conical connection and internal hex. Implants were placed with bone margin thickness: 0.0 mm, 0.2 mm, 0.3 mm, 0.4 mm, 0.5 mm, 0.6 mm, 0.7 mm, 0.9 mm, 1.1 mm, and 1.2 mm, respectively. X-ray markers made of dental composite were attached to each side of the bone model for accurate superimposition. Closed-tray impression transfers were attached to the implants (Figures 1 and 2).

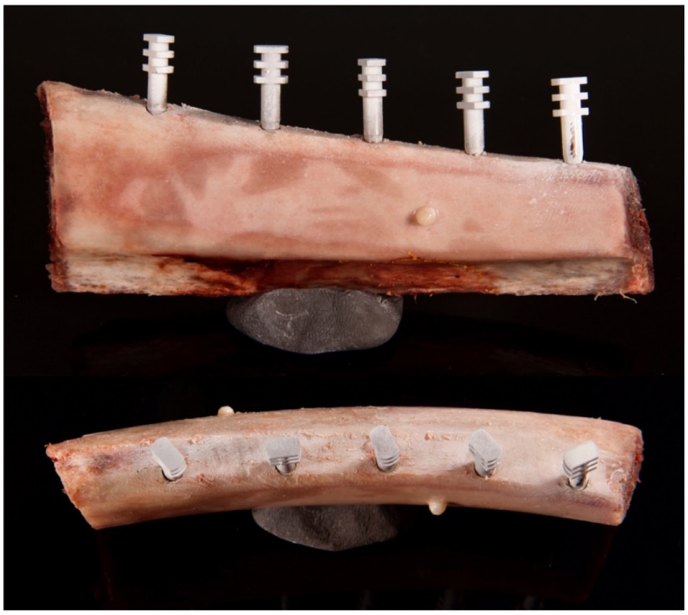

Figure 1. Bone model containing five implants with attached closed tray impression transfers coated with scan spray. Implants were placed with different bone margin thickness. X-ray markers made of dental composite were attached to the bone model surfaces.

Figure 2. Implant model with an attached closed tray impression transfer prepared for scanning.

An implant model consisting of the same dental implant with closed-tray impression transfer was also prepared (Figure 2). All metallic materials were coated with scan spray (Renfert, Germany) prior to scanning.

Two bone models and an implant-with-transfer model were scanned with 3shape model E4 (3shape, Denmark). The STL files of the scanned models were exported. Cone beam computed tomography images of two bone models were taken using Vatech Pax-i 3D (Vatech, Hwaseong, Korea). Sixteen CBCTs were taken of each implant with the following exposure parameters of voltage: 60, 70, 80, 90 kV; current: 4, 10 mA; and voxel size: 200, 300 µm. Metal artifact reduction was not used. In total, 160 separate images of dental implants were obtained. DICOM data of CBCT images were exported. Projects containing each bone model (STL), implant-with-transfer model (STL), and bone CBCT images (DICOM) were created using BlueSkyPlan planning software (Blue Sky Bio, Libertyville, IL, USA). All the data were superimposed using planning software and adjusted manually afterwards. A cross-section in the middle of each implant was obtained and CBCT scans were assessed using bone window settings (Figure 3).

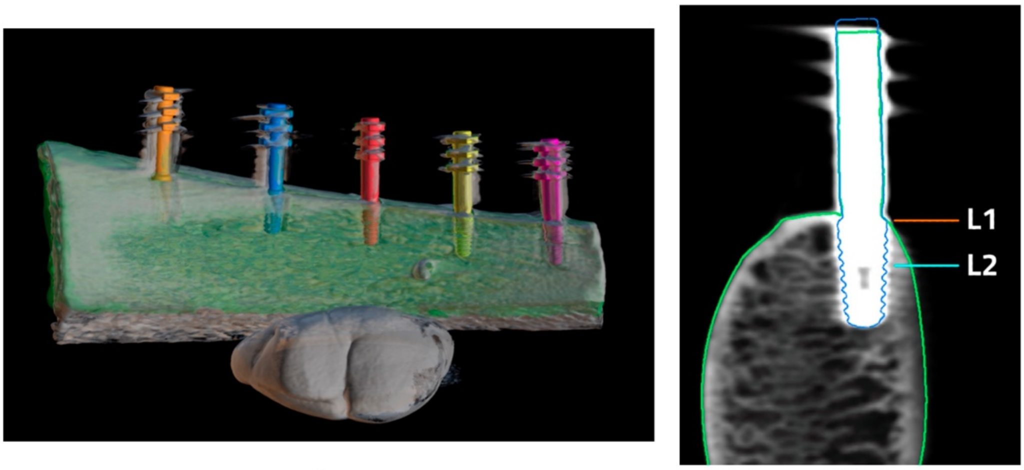

(**a**) (**b**)

Figure 3. Superimposed STL and DICOM files. (**a**) 3D reconstruction of superimposed DICOM FILES (gray), bone model (green), and implant-with-transfer models (orange, blue, red, yellow, purple); (**b**) Implant cross section, green outline—bone STL model, blue line—implant-with-transfer model. Bone margin measurement levels are marked as L1 (implant neck) and L2 (3.5 mm apically from implant neck).

Bone margin was measured in BlueSkyPlan planning software on cross sections using a digital distance measure tool in a horizontal plane at two levels: implant neck (L1) and 3.5 mm apically to implant neck (L2). The measurements on the scans were treated as ground truth. The measurements on CBCT images were performed at the same levels as ground truth. The mean squared error (MSE) being the squared differences between measurements was used in the accuracy assessment of CBCT. All measurements were performed twice. The interval between the first and the second reading was at least 6 weeks. The interval between first and second reading was 6 weeks to ensure that the measurements were repeatable and that there was no effect of the first reading on the second one. The intrarater reliability was assessed with the intra-class correlation coefficient (ICC) based on a 2-way mixed-effects mean-rating model. The mean from two measurements was taken into consideration in further statistical analysis. Study design is presented on the flowchart (Figure 4).

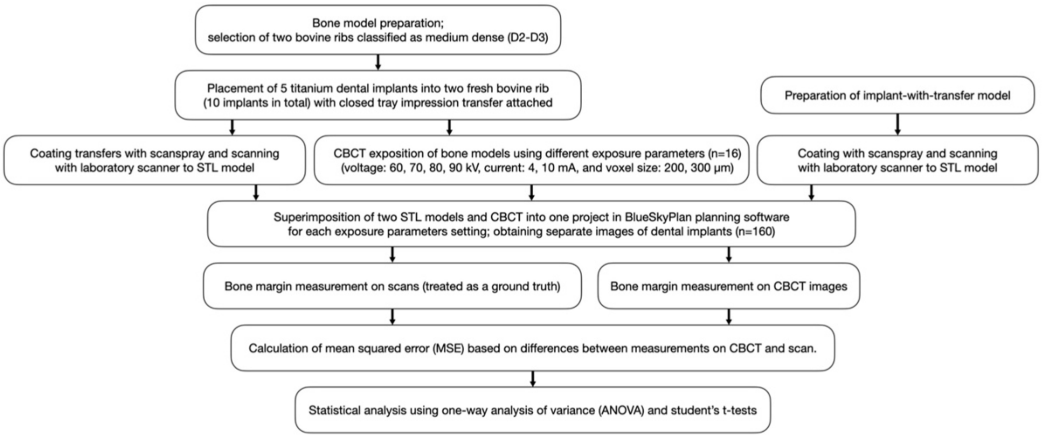

Figure 4. Study design flowchart.

A one-way analysis of variance (ANOVA) was used to assess the relationship between voltage and MSE, as well as implant position and MSE. Student's t-tests were performed for the assessment of current, voxel size, and MSE relationships. Linear regression was used to find the linear equation of relationship between the bone thickness and MSE for each voltage. According to this equation, the range of bone thicknesses was selected for each the MSE was less than 0.25 mm^2, which corresponds to the error of measurements of less than 0.5 mm.

3. Results

The mean values from ground truth measurements at both bone levels are presented in Table 1. The intrarater reliability was excellent in terms of repeatability of measurements (ICC = 94.1%).

Table 1. Measurements on the scans at two bone levels.

Implant	Mean of Two Measurements at Level 1 [mm]	Mean of Two Measurements at Level 2 [mm]
1	0.00	0.17
2	0.27	1.21
3	0.77	1.83
4	1.09	2.31
5	1.20	2.54
6	0.25	1.26
7	0.55	1.55
8	0.61	1.68
9	0.43	1.71
10	0.95	2.19

A significant relationship between the voltage and MSE of bone thickness measurement was observed (ANOVA, F = 2.75, p = 0.044), proving that the higher the voltage, the lower the MSE. Therefore, a higher voltage is better to reduce the measurement error caused by dental implant material (Table 2).

Table 2. Relationship between voltage and MSE of bone thickness measurements.

kV	MSE [mm^2]	SD of Error [mm^2]
60	0.27	0.35
70	0.18	0.22
80	0.18	0.19
90	0.14	0.14
All	0.19	0.23

kV—kilovolts, MSE—mean squared error, SD—standard deviation.

The relationship between implant position and MSE was also significant (ANOVA, $F = 2.74$, $p = 0.005$). No statistically significant results were observed for current (*t*-test, $p = 0.956$) or voxel size (*t*-test, $p = 0.055$) (Table 3).

Table 3. Voxel size and current assessment.

	Current			Voxel Size		
	4 mA	10 mA	*p*-Value	200 µm	300 µm	*p*-Value
mean MSE [mm^2]	0.18	0.18	0.969	0.20	0.15	0.055

The linear regression analysis revealed that accurate results for bone margin thickness can be obtained for voltage of 70, 80, and 90 kV. The higher the distance to measure, the higher the error. For 60 kV, the MSE is always above 0.25 in the measured range. The higher the voltage, the higher the threshold value of accurate measured distance and the more accurate measurements are feasible (Table 4).

Table 4. Linear regression results.

Voltage	Bone Margin Thickness for MSE < 0.25	*p*-Value	Regression Equation
60 kV	never		
70 kV	0.00–0.72	0.161	$0.17 \times d + 0.13$
80 kV	0.00–1.08	0.004	$0.21 \times d + 0.03$
90 kV	0.00–1.12	<0.001	$0.23 \times d + -0.01$
ALL	0.00–0.88	0.047	$0.13 \times d + 0.13$

d—bone margin thickness.

4. Discussion

This study confirms the thesis that dimensional error in the measurement of buccal bone thickness around dental implant depends on the voltage and dental implant position. The MSE decreases statistically significantly with increasing voltage and buccal bone width. There were statistically significant differences between current and voxel size values.

These results could have significant clinical implications. During follow-up of patients treated with dental implants, CBCT assessment raises concerns regarding the peri-implant bone thickness and the number of dental artifacts. This study suggests the possibility of decreasing the X-ray dose by setting parameters that do not affect the MSE, such as the voxel size and the intensity of the X-ray tube, at a level that allows the maximal reduction of the X-ray dose [26]. In addition, the awareness of limitations in peri-implant tissue measurement using CBCT requires thorough clinical examination before any intervention is undertaken.

We chose bovine ribs for this in vitro study to simulate alveolar bone. This type of human bone simulation was used previously in the literature on peri-implant bone defects or X-ray artifacts surrounding dental implants [29,31–35]. Bovine rib bone has cortical and cancellous bone of similar thickness and structure as a human mandible [36,37]. In their study, Bredbenner et al. assessed insertion and pull-out torque for 1.0 mm and 2.4 mm outer diameter screws for different substitutes for human cadaveric bone in maxillofacial rigid-fixation research. Although no single material was ideal, it was found that bovine rib could be the material of choice to simulate human cadaveric bone, but statistically significant differences ($p < 0.05$) were found between bovine bone and cadaveric group for pull-out strength [38]. The analysis of artifacts related to the different shape of the human mandible requires further studies. However, the effect of artifacts from the opposite side of the mandible is negligible compared to the beam hardening effect associated with the implant [32].

To the best of our knowledge, there are no studies with comparable measuring methods where the superimposition of the STL models and CBCT images were performed. In the available literature, measurements of buccal bone were performed by bone sounding using a blunt needle or measurement of buccal bone before implant placement or after implant removal [39,40]. The applied methodology allows for measurements of the implant, osseous tissue, and soft tissues in a selected area at any time that has passed since the scans and CBCT were performed. In the methods used until now, these were possible for a limited period of time due to the possibility of performing measurements only prior to implant placement, and the possible damage to the material during storage or after freezing. The main disadvantage of this approach using superimposition is the presence and intensity of artifacts related to X-ray markers or titanium abutments. Image distortion prevents automatic superimposition and requires manual adjustment, which extends the time of project preparation and may decrease its accuracy.

There have been several studies evaluating the accuracy of measurements around dental implants with similar methodologies involving measurements at the same level of bone plate thickness on a model and using CBCT. Wang et al. (2013) used CBCT to perform radiographic images of pigs' jaws with placed implants. They were cut at every implant site in the bucco-oral direction resulting in 40-µm sections that were stained with toluidine blue, measured, and then compared to CBCT images. Accuracy of -0.22 ± 0.77 mm for measurements on CBCT was observed [41]. Vanderstuyft et al. showed that there is a doubtful zone around a dental implant of about 0.45 mm. This means that buccal bone width below 0.45 mm may not always be observed in CBCT. Implant blooming percentage of up to 12–15% (increase of implant width in CBCT image) and an underestimation of the peri-implant buccal bone thickness, depending on the CBCT device used, by an average of 0.27 ± 0.19 mm (Accuitomo® 170, J. Morita, Kyoto, Japan) and 0.22 ± 0.17 mm (NewTom® VGi evo® (QR Verona, Verona, Italy) were found [39].

González-Martín et al. performed a study with three different computed tomography studies (1 CT and 2 CBCT devices) and reported that for sites with 0.5 mm buccal bone thickness, the probability of being radiographically visible was less than 20% and the odds of bone identification increased for a 1 mm increase in bone thickness. The mean distortion error for all CBCT devices was 0.39 mm [40]. There were no significant differences among the three devices [40]. Rezavi et al. observed an underestimation of buccal bone when it was thinner than 0.8 mm for both selected CBCT devices [42].

Based on the literature, we set the mean squared error at 0.25 in an arbitrary way for the statistical assessment of the dimensional distortion error under selected conditions. The MSE of 0.25 mm^2 corresponds to the 0.5 mm error in buccal bone measurement between a scan and the CBCT image.

Crestal bone loss following implant placement, as mentioned, is 0.24 ± 0.62 mm after one year. In the context of the results obtained, it is extremely important to properly set the exposure parameters when performing CBCT to determine the thickness of the vestibular bone plate. Despite high voltage value in a CBCT scan, in cases with thin buccal bone plate associated with severe bone loss, the presence of dimensional distortion error may suggest its complete resorption. However, in the case of thick buccal bone plate exposed with low value of voltage, the mean dimensional error may be greater than 0.5 mm, which can significantly distort the measurement result. In any of these situations, a significant measurement error of the buccal bone plate may lead the dentist to make an ill-informed decision about the need for surgical intervention to improve the amount of peri-implant tissue. Vanderstuyft et al. suggest measurements of the crestal peri-implant buccal bone thickness during implant placement surgery. With the baseline buccal bone thickness, implant diameter, and average implant blooming percentage or mean dimensional error as a reference, the subsequent decision on possible intervention is facilitated [39].

This study has several limitations that should be taken into consideration. The present study was conducted with a single CBCT device using several exposure parameters such as voltage, tube current, and voxel size. A study with the use of more CBCT devices might yield different results, especially when considered that the results of the relationship between voxel size and MSE ($p = 0.055$) were close to achieving a level of statistical significance. Secondly, no simulation of soft tissues was performed in this study. The novel methodology used in this study could be refined with the addition of a thin layer of wax to simulate soft tissues. This will require a digital scan of the model with and without a wax layer to further evaluate the ability to measure the thickness of soft and hard tissues.

The superimposition in BlueSkyPlan planning software could be done automatically or based on observer-defined landmarks (at least five). The best superimposition results could be obtained when landmarks on scan and X-ray models are repeatable and selected in three axes (transversal, antero-posterior, and vertical), keeping an appropriate distance between them. At first, in a pilot study, a scanbody was selected as an abutment attached to each implant instead of a closed-tray impression transfer. The main advantage of a scanbody is its matte surface, which facilitated the digital scanning, but there were issues with superimposition caused by its shape. The shape of a scanbody developed by the manufacturer of the implants used in the present study lacked defined edges enough to determine the same landmarks on a scan and X-ray model due to the artifacts caused by beam hardening on the X-ray model, as the scanbody was also made from titanium. A change from the scanbody to a closed-tray impression transfer and coating it with scanspray partially solved this problem, but it needed manual adjustment due to the presence of artifacts. Superimposition could be improved by selecting different abutment material, which should generate less artifacts in the CBCT image. For instance, it could be made individually using CAD/CAM from radiolucent material, such as polyetheretherketone (PEEK), with radiopaque x-ray markers [43].

Further studies are needed to verify these findings in a larger group of implants using different CBCT machines, exposure parameters (i.e., field of view), and considering the application of fresh human cadaver heads.

5. Conclusions

The voltage has an important impact on the accuracy of CBCT measurements. The higher the voltage, the lower the mean squared error of the measurements. The distortions of measurements depend on the thickness of the bone margin, and the higher the distance to measure, the higher the error. Bone margin thickness can be measured accurately (with an MSE of less than 0.25) for 70, 80, and 90 kV.

Author Contributions: Conceptualization, P.S. and P.R.; methodology, P.S. and P.R.; software, P.S. and A.W.; validation, P.R.; formal analysis, P.R.; investigation, P.S. and A.W.; resources, P.S.; data curation, P.S. and P.R.; writing—original draft preparation, P.S. and P.R.; writing—review and editing, P.R.; visualization, P.S.; supervision, P.R. and P.J.Z.; project administration, P.S.; funding acquisition, P.S. All authors have read and agreed to the published version of the manuscript.

Funding: This research received no external funding.

Data Availability Statement: Data generated or analysed during the study are available from the corresponding author on request.

Conflicts of Interest: The authors declare no conflict of interest.

References

1. An, X.; Oh, J.-H.; Jeong, S.-M.; Choi, B.-H. Natural bone healing in compromised sockets after tooth extraction: Digital measurement methods with cone-beam computed tomography. *J. Oral Implant.* **2021**, *47*, 236–241. [CrossRef] [PubMed]
2. Chappuis, V.; Engel, O.; Reyes, M.; Shahim, K.; Nolte, L.P.; Buser, D. Ridge alterations post-extraction in the esthetic zone: A 3D analysis with CBCT. *J. Dent. Res.* **2013**, *92*, 195s–201s. [CrossRef] [PubMed]
3. Araujo, M.G.; Sukekava, F.; Wennstrom, J.L.; Lindhe, J. Ridge alterations following implant placement in fresh extraction sockets: An experimental study in the dog. *J. Clin. Periodontol.* **2005**, *32*, 645–652. [CrossRef] [PubMed]
4. Avila-Ortiz, G.; Chambrone, L.; Vignoletti, F. Effect of alveolar ridge preservation interventions following tooth extraction: A systematic review and meta-analysis. *J. Clin. Periodontol.* **2019**, *46*, 195–223. [CrossRef] [PubMed]
5. Buser, D.; Janner, S.F.M.; Wittneben, J.-G.; Brägger, U.; Ramseier, C.A.; Salvi, G.E. 10-year survival and success rates of 511 titanium implants with a sandblasted and acid-etched surface: A retrospective study in 303 partially edentulous patients. *Clin. Implant Dent. Relat. Res.* **2012**, *14*, 839–851. [CrossRef]
6. Monje, A.; Chappuis, V.; Monje, F.; Muñoz, F.; Wang, H.-L.; Urban, I.; Buser, D. The critical peri-implant buccal bone wall thickness revisited: An experimental study in the beagle dog. *Int. J. Oral Maxillofac. Implant.* **2019**, *34*, 1328–1336. [CrossRef]
7. Maier, F.-M. Initial crestal bone loss after implant placement with flapped or flapless surgery—A prospective cohort study. *Int. J. Oral Maxillofac. Implant.* **2016**, *31*, 876–883. [CrossRef]
8. Berglundh, T.; Armitage, G.; Araujo, M.G.; Avila-Ortiz, G.; Blanco, J.; Camargo, P.M.; Chen, S.; Cochran, D.; Derks, J.; Figuero, E.; et al. Peri-implant diseases and conditions: Consensus report of workgroup 4 of the 2017 World Workshop on the Classification of Periodontal and Peri-Implant Diseases and Conditions. *J. Periodontol.* **2018**, *89*, S313–S318. [CrossRef]
9. Papapanou, P.N.; Sanz, M.; Buduneli, N.; Dietrich, T.; Feres, M.; Fine, D.H.; Flemmig, T.F.; Garcia, R.; Giannobile, W.V.; Graziani, F.; et al. Periodontitis: Consensus report of workgroup 2 of the 2017 World Workshop on the Classification of Periodontal and Peri-Implant Diseases and Conditions. *J. Periodontol.* **2018**, *89*, S173–S182. [CrossRef]
10. Abrahamsson, I.; Soldini, C. Probe penetration in periodontal and peri-implant tissues: An experimental study in the beagle dog. *Clin. Oral Implant. Res.* **2006**, *17*, 601–605. [CrossRef]
11. Bohner, L.; Habor, D.; Tortamano, P.; Radermacher, K.; Wolfart, S.; Marotti, J. Assessment of buccal bone surrounding dental implants using a high-frequency ultrasound scanner. *Ultrasound Med. Biol.* **2019**, *45*, 1427–1434. [CrossRef] [PubMed]
12. Song, D.; Shujaat, S.; Vasconcelos, K.D.F.; Huang, Y.; Politis, C.; Lambrichts, I.; Jacobs, R. Diagnostic accuracy of CBCT versus intraoral imaging for assessment of peri-implant bone defects. *BMC Med. Imaging* **2021**, *21*, 23. [CrossRef] [PubMed]
13. Mohan, R.; Mark, R.; Gundappa, M.; Balaji, M.D.S.; Vijay, V.; Umayal, M. Comparative evaluation of periodontal osseous defects using direct digital radiography and cone-beam computed tomography. *J. Pharm. Bioallied Sci.* **2021**, *13*, S306–S311. [CrossRef] [PubMed]
14. Ruetters, M.; Hagenfeld, D.; ElSayed, N.; Zimmermann, N.; Gehrig, H.; Kim, T.-S. Ex vivo comparison of CBCT and digital periapical radiographs for the quantitative assessment of periodontal defects. *Clin. Oral Investig.* **2020**, *24*, 377–384. [CrossRef] [PubMed]
15. Palkovics, D.; Mangano, F.G.; Nagy, K.; Windisch, P. Digital three-dimensional visualization of intrabony periodontal defects for regenerative surgical treatment planning. *BMC Oral Health* **2020**, *20*, 351. [CrossRef]
16. Woelber, J.P.; Fleiner, J.; Rau, J.; Ratka-Krüger, P.; Hannig, C. Accuracy and usefulness of CBCT in periodontology: A systematic review of the literature. *Int. J. Periodontics Restor. Dent.* **2018**, *38*, 289–297. [CrossRef]
17. Golubovic, V.; Mihatovic, I.; Becker, J.; Schwarz, F. Accuracy of cone-beam computed tomography to assess the configuration and extent of ligature-induced peri-implantitis defects. A pilot study. *Oral Maxillofac. Surg.* **2012**, *16*, 349–354. [CrossRef]
18. Jacobs, R.; Salmon, B.; Codari, M.; Hassan, B.; Bornstein, M.M. Cone beam computed tomography in implant dentistry: Recommendations for clinical use. *BMC Oral Health* **2018**, *18*, 88. [CrossRef]
19. Jacobs, R.; Vranckx, M.; Vanderstuyft, T.; Quirynen, M.; Salmon, B. CBCT vs other imaging modalities to assess peri-implant bone and diagnose complications: A systematic review. *Eur. J. Oral Implantol.* **2018**, *11*, 77–92.
20. Hussain, R.A.; Miloro, M.; Cohen, J.B. An update on the treatment of periimplantitis. *Dent. Clin. N. Am.* **2021**, *65*, 43–56. [CrossRef]
21. Kayal, R.A. Distortion of digital panoramic radiographs used for implant site assessment. *J. Orthod. Sci.* **2016**, *5*, 117–120. [CrossRef] [PubMed]
22. Suphangul, S.; Rattanabanlang, A.; Amornsettachai, P.; Wongsirichat, N. Dimension distortion of digital panoramic radiograph on posterior mandibular regions. *Mahidol Dent. J.* **2016**, *36*, 279–286.
23. Greenstein, G.; Cavallaro, J.S., Jr.; Tarnow, D.P. Clinical pearls for surgical implant dentistry: Part I. *Dent. Today* **2010**, *29*, 124–127.
24. Coelho-Silva, F.; Gaêta-Araujo, H.; Rosado, L.P.L.; Freitas, D.Q.; Haiter-Neto, F.; De-Azevedo-Vaz, S.L. Distortion or magnification? An in vitro cone-beam CT study of dimensional changes of objects with different compositions. *Dentomaxillofac. Radiol.* **2021**, *50*, 20210063. [CrossRef]
25. Schulze, R.K.W.; Berndt, D.; D'Hoedt, B. On cone-beam computed tomography artifacts induced by titanium implants. *Clin. Oral Implant. Res.* **2010**, *21*, 100–107. [CrossRef] [PubMed]
26. Sawicki, P.; Zawadzki, P.J.; Regulski, P. The Impact of cone-beam computed tomography exposure parameters on peri-implant artifacts: A literature review. *Cureus* **2022**, *14*, 23035. [CrossRef]

27. Commission, E. Cone Beam CT for Dental and Maxillofacial Radiology. In *Evidence-Based Guidelines*; Radiation Protection No. 172; European Commission: Luxemburg, 2012.
28. Aljohani, M.; Yong, S.L.; Bin Rahmah, A. The effect of surgical regenerative treatment for peri-implantitis: A systematic review. *Saudi Dent. J.* **2020**, *32*, 109–119. [CrossRef]
29. Falco, A.; Berardini, M.; Trisi, P. Correlation between implant geometry, implant surface, insertion torque, and primary stability: In vitro biomechanical analysis. *Int. J. Oral Maxillofac. Implant.* **2018**, *33*, 824–830. [CrossRef]
30. Misch, C. Bone character: Second vital implant criterion. *Dent. Today* **1988**, *7*, 39–40.
31. Saberi, B.V.; Khosravifard, N.; Ghandari, F.; Hadinezhad, A. Detection of peri-implant bone defects using cone-beam computed tomography and digital periapical radiography with parallel and oblique projection. *Imaging Sci. Dent.* **2019**, *49*, 265–272. [CrossRef]
32. Schwindling, F.S.; Hilgenfeld, T.; Weber, D.; Kosinski, M.A.; Rammelsberg, P.; Tasaka, A. In vitro diagnostic accuracy of low-dose CBCT for evaluation of peri-implant bone lesions. *Clin. Oral Implant. Res.* **2019**, *30*, 1200–1208. [CrossRef] [PubMed]
33. Eskandarloo, A.; Saati, S.; Ardakani, M.P.; Jamalpour, M.; Mezerji, N.M.G.; Akheshteh, V. Diagnostic accuracy of three cone beam computed tomography systems and periapical radiography for detection of fenestration around dental implants. *Contemp. Clin. Dent.* **2018**, *9*, 376–381. [CrossRef] [PubMed]
34. de-Azevedo-Vaz, S.L.; Peyneau, P.; Ramirez-Sotelo, L.; de Faria Vasconcelos, K.; Campos, P.S.F.; Haiter-Neto, F. Efficacy of a cone beam computed tomography metal artifact reduction algorithm for the detection of peri-implant fenestrations and dehiscences. *Oral Surg. Oral Med. Oral Pathol. Oral Radiol.* **2016**, *121*, 550–556. [CrossRef] [PubMed]
35. Dong, T.; Yuan, L.; Liu, L.; Qian, Y.; Xia, L.; Ye, N.; Fang, B. Detection of alveolar bone defects with three different voxel sizes of cone-beam computed tomography: An in vitro study. *Sci. Rep.* **2019**, *9*, 8146. [CrossRef]
36. Chiodo, T.A.; Ziccardi, V.B.; Janal, M.; Sabitini, C. Failure strength of 2.0 locking versus 2.0 conventional Synthes mandibular plates: A laboratory model. *J. Oral Maxillofac. Surg.* **2006**, *64*, 1475–1479. [CrossRef]
37. Choi, B.-H.; Huh, J.-Y.; Suh, C.-H.; Kim, K.-N. An in vitro evaluation of miniplate fixation techniques for fractures of the atrophic edentulous mandible. *Int. J. Oral Maxillofac. Surg.* **2005**, *34*, 174–177. [CrossRef] [PubMed]
38. Bredbenner, T.L.; Haug, R.H. Substitutes for human cadaveric bone in maxillofacial rigid fixation research. *Oral Surg. Oral Med. Oral Pathol. Oral Radiol. Endodontol.* **2000**, *90*, 574–580. [CrossRef]
39. Vanderstuyft, T.; Tarce, M.; Sanaan, B.; Jacobs, R.; Vasconcelos, K.D.F.; Quirynen, M. Inaccuracy of buccal bone thickness estimation on cone-beam CT due to implant blooming: An ex-vivo study. *J. Clin. Periodontol.* **2019**, *46*, 1134–1143. [CrossRef]
40. Gonzalez-Martin, O.; Oteo, C.; Ortega, R.; Alandez, J.; Sanz, M.; Veltri, M. Evaluation of peri-implant buccal bone by computed tomography: An experimental study. *Clin. Oral Implant. Res.* **2016**, *27*, 950–955. [CrossRef]
41. Wang, D.; Künzel, A.; Golubovic, V.; Mihatovic, I.; John, G.; Chen, Z.; Becker, J.; Schwarz, F. Accuracy of peri-implant bone thickness and validity of assessing bone augmentation material using cone beam computed tomography. *Clin. Oral Investig.* **2013**, *17*, 1601–1609. [CrossRef]
42. Razavi, T.; Palmer, R.M.; Davies, J.; Wilson, R.; Palmer, P.J. Accuracy of measuring the cortical bone thickness adjacent to dental implants using cone beam computed tomography. *Clin. Oral Implant. Res.* **2010**, *21*, 718–725. [CrossRef] [PubMed]
43. Lo Giudice, R.; Sindoni, A.; Tribst, J.P.M.; de Oliveira Dal Piva, A.M.; Lo Giudice, G.; Bellezza, U.; Lo Giudice, G.; Famà, F. Evaluation of zirconia and high-performance polymer abutment surface roughness and stress concentration for implant-supported fixed dental prostheses. *Coatings* **2022**, *12*, 238. [CrossRef]

Cureus

Open Access Review Article

DOI: 10.7759/cureus.23035

The Impact of Cone-Beam Computed Tomography Exposure Parameters on Peri-Implant Artifacts: A Literature Review

Review began 02/11/2022
Review ended 02/28/2022
Published 03/10/2022

Paweł Sawicki [1] , Paweł J. Zawadzki [1] , Piotr Regulski [2, 3]

1. Department of Cranio-Maxillofacial Surgery, Oral Surgery, and Implantology, Medical University of Warsaw, Warsaw, POL 2. Department of Dental and Maxillofacial Radiology, Medical University of Warsaw, Warsaw, POL 3. Center of Digital Science and Technology, Cardinal Stefan Wyszyński University in Warsaw, Warsaw, POL

Corresponding author: Piotr Regulski, piotr.regulski@wum.edu.pl

Abstract

Cone-beam computed tomography (CBCT) amounts to an excellent diagnostic tool to evaluate the peri-implant bone thickness in all dimensions. Despite the unquestionable advantages of CBCT, potential artifacts around dental implants might disturb the proper assessment of the surrounding structures. The artifacts may mask osseointegration, shallow bone defects, and other types of radiolucency, which make it difficult to establish an early diagnosis of bone loss. Proper diagnosis of bone defect is necessary to decide about surgical intervention. The aim of this literature review is to assess the CBCT exposure causing artifacts on the peri-implant structures. An electronic search of MEDLINE (PubMed) database includes studies published before July 2021 and supplemented by manual research. Clinical, ex vivo, in vitro, and animal studies evaluating the relationship between exposition parameters and occurrence of artifacts around the dental implant in CBCT studies were included. A literature review revealed that kilovoltage, tube current, and field of view may affect the occurrence of artifacts around dental implants, all of which would compromise radiological evaluation. Therefore, it is feasible to reduce the incidence of artifacts and improve the image quality by appropriate modification of the exposure parameters. However, the reduction of artifacts is often associated with a significant increase in radiation exposure; hence, an effort should be made to minimize the radiation dose in line with the ALARA (as low as reasonably achievable) principle.

Categories: Radiology, Dentistry
Keywords: radiation protection, dental implants, radiation, metal artifacts, cbct

Introduction And Background

Nowadays, dental implants are the best and increasingly popular method for replacing missing teeth. Planning implant treatment requires detailed diagnosis, especially in terms of bone quantity and quality. Panoramic and periapical radiography is used as a preoperative diagnostic radiological method. Its constraints, such as overlapping structures and the lack of possibility to assess bone volume, limit the preimplantation treatment planning. Nowadays, cone-beam computed tomography (CBCT) allows for a three-dimensional assessment of the quality and volume of bone tissue at reasonable cost and dose and remains the gold standard [1]. In modern CBCT devices, with an appropriate setting of exposure parameters, the effective dose is relatively small and expected to be 70 µSv for a field of view of 8 cm x 8 cm and 121 µSv for a field of view of 15 cm x 15 cm [2].

Patients after implant placement are at the risk of peri-implantitis, which might, in turn, lead to the loss of the dental implant. A systematic literature review among patients with fixed partial dentures showed that the prevalence of peri-implantitis was 9.6% in the general population and 14.3% among patients with periodontal disease [3]. Peri-implantitis is usually a chronic condition, which might lead to advanced bone loss, especially in the absence of regular, postoperative follow-ups. Effective diagnosis is of great importance when considering surgical intervention. Despite the advantages of CBCT, the authors point to the masking of the osseointegration, shallow bone defects, and other types of radiolucency, which makes it difficult to establish an early diagnosis of bone loss. This is caused by the presence of artifacts, i.e., parts of the image that do not represent any anatomical structure within the subject being evaluated and might be most commonly generated around the radiodense elements in a radiographic image [1].

CBCT images might contain various types of artifacts such as beam hardening phenomenon, photon starvation, scatter, partial volume effect, undersampling, exomass, detector miscalibration, and patient motion [4]. Exposure of objects containing metals from which dental implants are made is associated with the formation of artifacts that reduce image quality. They might disturb proper assessment of the surrounding structures [5].

Beam hardening phenomenon and photon starvation are the main causes of peri-implant artifacts. Beam hardening occurs when a polychromatic x-ray beam passes through an object, resulting in selective absorption of lower energy (lower wavelength) photons and thus increased beam energy [6]. The higher the

How to cite this article
Sawicki P, Zawadzki P J, Regulski P (March 10, 2022) The Impact of Cone-Beam Computed Tomography Exposure Parameters on Peri-Implant Artifacts: A Literature Review. Cureus 14(3): e23035. DOI 10.7759/cureus.23035

density and the atomic number of an object, the higher the number of absorbed photons [7]. The mechanism underlying CBCT artifacts is the same as the one in computed tomography (CT). However, artifacts are more prominent in CBCT compared to CT due to the lower tube voltage [5]. Two types of artifacts are generated as a result of beam hardening: cupping artifacts, caused by a non-linear x-ray beam attenuation and dark bands or streaks between highly dense objects (Figures *1*, *2*) [8].

FIGURE 1: Beam hardening artifacts adjacent to metal post and core in anterior maxillary tooth

Image credit: The authors of the current study.

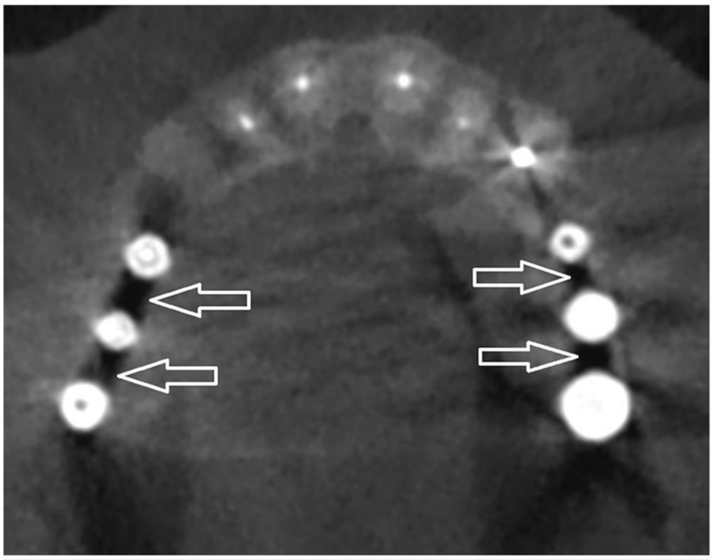

FIGURE 2: Dark streaks between dental implants in cone-beam computed tomography (type of beam hardening artifacts)

Image credit: The authors of the current study.

Photon starvation in CBCT often occurs around prosthetic crowns and implants. When the x-ray beam is traveling horizontally, the attenuation is greatest, e.g., when it passes through very dense objects. This generates a large amount of noise and streak artifacts around highly saturated objects (Figure 3) [9]. Effects similar to the ones seen for beam hardening and photon starvation are caused by scattering.

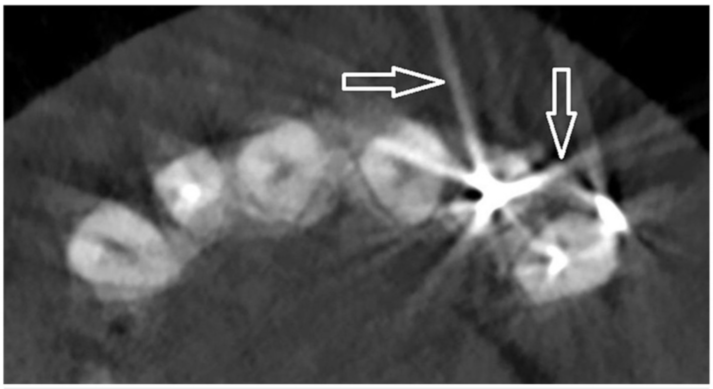

FIGURE 3: Photon starvation effect generates a large amount of noise and streaks around metal post and core in the anterior maxillary tooth

Image credit: The authors of the current study.

The main objective of this article is to provide an in-depth discussion on the impact of CBCT exposure parameters on peri-implant assessment feasibility taking into consideration the available literature. In the vast majority of CBCT machines, all exposure parameters can be set manually within a given range. This not only allows to change the dose of absorbed radiation but also influences the incidence of artifacts in the field of view (FOV). In clinical practice, the quality of CBCT images depends on multiple factors, such as machine model, FOV, type of object scanned, exposure time, x-ray tube voltage, and tube current as well as spatial resolution defined by the size of the imaging voxels [10]. Furthermore, manufacturers offer a metal artifact reduction tool (MAR) based on a reconstruction algorithm [11]. MAR software activation reduces the interference caused by metals and may improve the image quality [12].

Review

Search strategy and selection criteria

The main objective of this article is to analyze the impact of designated CBCT exposure parameters on the inherent peri-implant artifacts taking into consideration the available literature. The MEDLINE (PubMed) bibliographic database was searched for studies published before July 2021 and supplemented by manual research. The search strategy was restricted to English language publications using the following combined terms: (dental OR dentistry) AND implant AND (artifacts OR artifacts).

Studies and reviews evaluating the relationship between exposition parameters and occurrence of artifacts around the dental implant in CBCT studies were included. Titles and abstracts were screened based on the inclusion criteria. Case reports were not included. Publications not fulfilling the eligibility criteria were not included in this analysis. During the procedure, studies for which full texts could not be obtained were excluded. The full text of the selected papers was reviewed, and the relevant data on the impact of exposure parameters on peri-implant artifacts were extracted.

After removing duplicates, references were screened, and 378 titles were found and considered eligible for further consideration. A total of 284 titles were excluded based on title evaluation. Initial review of the abstracts resulted in 72 articles that were considered for full-text review. A total of 35 papers had to be excluded at this stage because they did not fulfill the inclusion criteria. Nine additional records identified through the manual search were included. Forty-six articles were included in the present review. Figure *4* shows a detailed flowchart of the literature review search and selection process according to the Preferred Reporting Items for Systematic Reviews and Meta-analyses (PRISMA) statement.

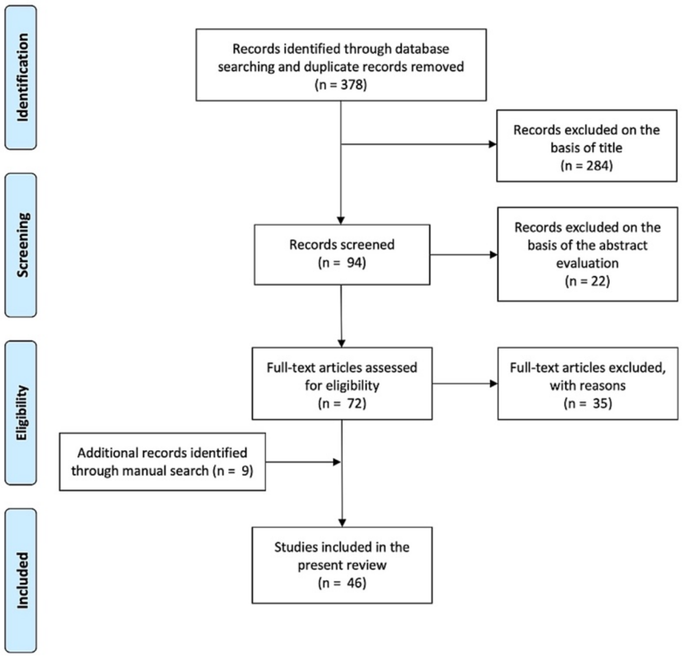

FIGURE 4: PRISMA diagram of the included studies

The image shows the selection process for the studies included according to the PRISMA statement.

PRISMA: Preferred Reporting Items for Systematic Reviews and Meta-analyses.

X-ray tube voltage and tube current

Low x-ray beam energy, high density of materials, and a high atomic number of the scanned object contribute to beam hardening [7,13]. Increasing the x-ray tube voltage increases the beam energy and improves x-ray penetration, resulting in image contrast and noise reduction as well as in the irradiation dose increment [5,13,14]. This leads to the reduction of the overall number of beam hardening artifacts (increased contrast-to-noise ratio [CNR]) [11,13]. However, the number of scatter artifacts caused by the photons with different energies increases in the low-voltage images [15]. Therefore, it is advisable to set the exposure parameters in a compromising manner to get an optimal reduction of both beam hardening and scatter. Beam hardening artifacts and scatter are present in each CBCT image but with a different intensity depending on x-ray voltage. A high x-ray value (e.g., 90 kV) allows to reduce the following artifacts but increases the radiation dose. Therefore, it is difficult to determine the ideal value of x-ray tube voltage. The authors of this article conducted studies aiming to determine the ideal x-ray tube voltage for postoperative implant therapy follow-up. Panjnoush et al. showed that a change in the tube voltage from 70 kVp to 84 kVp had no effect on the presence of artifacts in the spaces between metallic objects in dental applications [16]. It was shown that the incidence of artifacts for zirconium implants is higher compared to that of titanium implants. The reason for higher artifacts occurrence with zirconium implants is the difference in the atomic number of zirconium (Zr, atomic number = 40) and titanium (Ti, atomic number = 22), as shown in the previous part of the article [11].

The difference in the number of artifacts generated as a result of changes in the tube voltage is shown in Figure *5*. A bone model with a dental implant was exposed to tube voltages of 60 kV and 90 kV with constant other exposure parameters. Exposure to 60 kV significantly limited the diagnosis of peri-implant buccal plate defects.

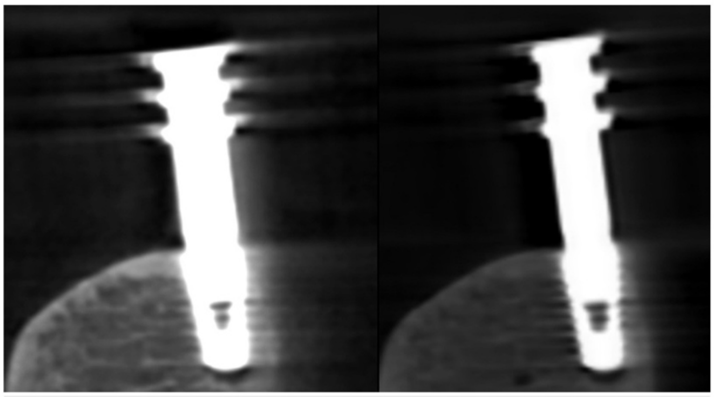

FIGURE 5: Bone model with a dental implant with impression transfer attached exposed to a tube voltage of 60 kV (left) and 90 kV (right)

The remaining exposure parameters are constant. Lower voltage limits the diagnosis of peri-implant buccal plate defects.

Image credit: The authors of the current study.

The cathode tube current has a significant influence on the radiation dose during CBCT exposure. An increase in mAs (the product of the lamp tube current and the exposure time) reduces the noise but increases the radiation dose [14]. Studies showed no effect of changes in the tube current (within the range available in the CBCT) on the formation of peri-implant artifacts [16-18]. In another study, Fontenele et al. found that a change in the tube current and metal artifact reduction algorithms (MAR) did not affect the diagnostic efficacy for vertical root fractures in endodontically treated teeth adjacent to zirconium implants [19].

Field of view

Increasing the FOV exposes more tissues to x-rays, increases scattered radiation to the surrounding tissues, decreases contrast, and increases noise and radiation dose [14,20,21]. Scatter might be reduced by reducing FOV as well as the use of an anti-scatter grid and algorithms to correct the x-ray scatter [22]. Pauwels et al., who investigated the relationship between FOV and the range of rotation and an effective dose of radiation, showed that the effective dose ranged from 54 µSv for 4 cm x 4 cm to 303 µSv for 17 cm x 12 cm when using Accuitomo 170 3D CBCT system (J. Morita Corporation, Japan) [20]. It was shown that artifacts are less prominent in a small FOV, which might be due to the fact that by an increase in FOV, the irradiated area increases in size, and consequently, scattered radiation, noise, and image artifact increase. Similar results were provided by Parsa et al. [17,23]. Nikbin et al. assessed the effect of an object position in the FOV and the use of the MAR algorithm on CBCT diagnostic efficacy in vertical root fractures. Diagnostic accuracy was higher with central positioning compared to peripheral positioning, irrespective of MAR [24].

It is recommended in clinical practice to limit the FOV, if possible, to avoid scanning areas susceptible to beam hardening (such as metal restorations and implants). If the target volume is too large, it might limit the diagnostic possibilities in the region of interest (ROI) due to the overlapping of artifacts outside this region. This can be achieved by collimating the beam, changing the patient's position, and separating the dental arches during CBCT scanning [25].

CBCT rotation range

The range of tube-detector axis rotation varies depending on the CBCT system and can be changed from 180 to 360 degrees in some systems [20]. CBCT scanning with 360-degree rotation compared to the standard 180-degree scan enhances the image quality by creating more basis images. Enhancement of rotation range increases the CNR, but despite the larger amount of data, changing the device rotation range does not affect the number of artifacts (e.g., beam hardening, scatter, and ring artifacts) that occur both in 180- and 360-degree scans [7,21,26].

Increasing the range of rotation extends the exposure time, which largely determines the effective dose of x-rays. The recommendations of radiological protection in CBCT, International Commission on Radiological Protection (ICRP) Publication 129, suggest a rotation of 180° plus beam angle rotation as sufficient for tomographic reconstruction. Radiosensitive organs should be on the detector side to reduce the risk of overexposure. A full, 360-degree rotation makes it impossible to avoid exposure to these structures [27].

Voxel size

A voxel is the smallest isotropic element of a CBCT image. CBCT devices allow for setting a voxel size from a minimum of 70 to 300 microns. The voxel size determines how small objects can be differentiated and how detailed diagnosis of maxillofacial anatomical structures can be performed [28]. The partial volume effect is an artifact associated with the voxel size. It occurs when two structures are projected on the same voxel producing an intensity value being an average value of both structures [29]. In consequence, these structures cannot be differentiated and the signal-to-noise ratio (SNR) for each voxel is reduced.

Research findings on the effect of voxel size on implant assessment are contradictory. Vasconcelos et al. assessed the differences in generating artifacts using zirconium and titanium implants placed in human mandibles (ex vivo) and different tube voltage and voxel size (high resolution, 0.16 mm; low resolution, 0.32 mm) [11]. It was shown that a reduced voxel size did not affect beam hardening and scatter artifact generation [13]. In the in vitro study using an I-CAT 3D Imaging System (Imaging Sciences International, Hatfield, PA), Kursun-Cakmak et al. assessed the image quality with different voxel sizes (0.2, 0.25, 0.3, and 0.4 mm) and recommended follow-up CBCT using low-resolution settings (0.3 and 0.4 mm) due to the highest CNR. The author also found that among the implant materials tested (zirconium (Zr), titanium Grade 4 [Ti], and titanium-zirconium [$Ti\text{-}ZrO_2$] alloy), titanium Grade 5 (titanium-aluminum-vanadium alloy) had the lowest impact on artifact creation, while Zr had the highest impact [30]. Bechara et al. found that the CNR value does not depend only on the voxel size but might vary for different CBCT systems. They found that a smaller voxel size does not guarantee an improved quality [26]. To summarize the following research results, it can be concluded that although reducing the size of the voxel increases spatial resolution, it also causes a deterioration of the image quality around dental implants and an unjustified increase in the radiation dose [1,14,18,26,30-32].

Software methods used to reduce artifacts

There are some software solutions that allow for the reduction of artifacts present in the acquired image, which improves its quality. Activation of the MAR algorithm, i.e., iterative reconstruction methods that allow reducing image interference is caused by metals or high-density objects by increasing the CNR [11,31,33]. The efficacy of MAR depends on the manufacturer of the radiographic machine [34]. In one study, cylinders made of titanium (Ti) and chromocobalt alloy (CrCo) were exposed to two CBCT devices: Picasso Trio (Vatech, South Korea) and ProMax (Planmeca, Helsinki, Finland). It was shown that the use of MAR for Ti cylinders significantly reduced the voxel's mean ($p \leqslant .05$) in the Picasso Trio CBCT machine and significantly increased the voxel's mean ($p \leqslant .05$) in the ProMax CBCT machine. No efficacy of MAR was demonstrated for CrCo cylinders using both machines [35]. Statistically significant ($p \leqslant 0.0001$) efficacy of MAR in reducing amalgam, copper-aluminum alloy, and titanium artifacts was found for various CBCT machines. The relationship between the atomic number of the metal and the increased number of artifacts was confirmed. It was found that a higher metal atomic number caused greater artifact expression [36].

Nascimento et al. investigated differences in the efficacy of MAR in three tested conditions: "without MAR," with "MAR activated after the acquisition," and with "MAR activated before the acquisition." For this purpose, a zirconium oxide implant was placed in the human mandibular bone at the position of the missing lower right first molar, and exposition was performed with the OP300 Maxio system (Instrumentarium Dental Inc., Tuusula, Finland). It was shown that the cortical lingual plate had lower CNR and voxel value in the control and the implant group ($p < 0.05$). It was demonstrated that MAR efficacy increased with an increasing number of artifacts. No relationship was found between MAR efficacy and its activation mode [4]. It was shown that the availability of more data (images from different projections also called basis images) increases the effectiveness of MAR. The relationship between the higher number of basis images and reduced generation of artifacts in the absence of activated MAR algorithms was not shown [37,38].

Kamburoglu et al. assessed the efficacy of MAR algorithms in the diagnosis of buccal peri-implant defects. To this end, buccal peri-implant defects were performed in implants placed into human cadaver mandibles and then investigated with CBCT in artifact reduction mode at four different levels of intensity, including the non-activated mode. It was shown that there is a statistically significant influence of MAR (regardless of its mode) on the diagnosis of simulated bone loss in the applied methodology. There was a higher interobserver agreement for periodontal defects (kappa value from 0.189 to 1.000) vs. peri-implant defects (kappa value from 0.140 to 0.792). It was also found that buccal peri-implant defects are more diagnostically challenging than buccal periodontal ones. The main cause of these is the presence of artifacts related to the metal around titanium dental implants, which does not occur in periodontal assessment because of the lack of metal in tooth structures despite the teeth being after endodontic treatment and treatment with metallic post and core restorations [39]. A similar study by de-Azevedo-Vaz et al. showed no improvement in the efficacy of diagnostic assessment of peri-implant fenestration and dehiscence using MAR [40]. In their study, Bechara et al. used ProMax and Master 3D (Vatech, Hwaseong, Republic of Korea) systems to assess the efficacy of artifact reduction algorithms in the diagnosis of root fractures in endodontically treated teeth. Both machines showed higher diagnostic sensitivity and specificity for vertical root fractures when using no AR [41].

Discussion

The foregoing article sums up for the first time the influence of all the variable parameters of CBCT device exposition in the presence of artifacts around dental implants. To date, the influence of the changing exposure parameters on the possibility of evaluation of the buccal bone around dental implants has not been determined. The authors of this document are conducting studies aiming to clarify this dependency, which will have a significant impact on the possibility of regular inspection for the implant and prosthetic treatment patients. The goal of the research is the discovery of the optimal image quality settings for the exposure parameters while maintaining the lowest dose of radiation possible.

Peri-implantitis and its predictable diagnostics in CBCT images are the main areas of interest in implantology. Peri-implantitis causes gradual destruction of osseous tissue around dental implants, which can lead to loss of implants. Appropriate postoperative care and diagnostics, both clinical as well as radiological, allow for assessment of peri-implant tissues and possible implementation of treatment during the early stages of the disease. Based on the results presented above, modifications to the exposure parameters of CBCT examinations performed during postoperative follow-up are recommended, which will allow for reduction of artifacts (mainly beam hardening effects) that prevent the assessment of osseous tissue around dental implants.

The x-ray tube voltage has a major influence on the occurrence of artifacts around dental implants and metal objects in CBCT images. Increasing x-ray tube voltage decreases the occurrence of artifacts such as beam hardening and noise and increases the CNR. Increasing the tube current decreases noise but does not affect the formation of artifacts around dental implants (peri-implant artifacts). Increasing the CBCT rotation range from 180 to 360 degrees does not affect the number of artifacts, and decreasing the voxel size does not improve the image quality around dental implants. To reduce scatter artifacts, the FOV should be reduced, if possible, which will both improve the image quality and reduce radiation dose. Following modifications of exposure parameters and their impact on CBCT image and radiation dose are detailed in Table *1*.

Exposure parameter	Artifacts (beam hardening)	Noise	Contrast-to-noise ratio (CNR)	Spatial resolution	Radiation dose
Voltage ↑	↓ [11,13]	↓ [14]	↑ [11,13]	-	↑ [14]
mAs ↑	-	↓ [14]	-	-	↑ [14]
Voxel size ↑	-	↓ [14,18,26,30,31]	-	↓ [28]	↓ [1,32]
Field of view ↑	↑ [17,23]	↑ [14,21]	↓ [14,21]	↓ [42]	↑ [14,21]
Rotation arc ↑	-	-	↑ [26]	-	↑ [27]
Metal artifact reduction	-	↓ [22,42,43]	↑ [11,31,33]	-	-

TABLE 1: Influence of exposure parameters modification on the incidence of artifacts and cone-beam computed tomography (CBCT) image quality

↑: Increase; ↓: Decrease; mAs: Tube current-exposure time product; kV: Tube voltage; MAR: Metal artifact reduction.

Taking into account the fact that modification of all above-mentioned parameters influences the radiation dose, only x-ray tube voltage and FOV should be modified, which are the only ones listed to influence the formation of peri-implant artifacts, leaving the other exposure parameters at settings that allow obtaining the lowest possible radiation dose. It is related to the ALARA (as low as reasonably achievable) principle proposed by the ICRP [44]. Although the principle seems commonly known, studies conducted in Turkey by Atci et al. indicate that 96% of the surveyed emergency medicine doctors and neurosurgeons of the local hospital in Istanbul did not know the meaning of the acronym ALARA, and 92% did not know the radiation doses received by their patients during brain CT [45]. As it is commonly known, the effective dose of x-ray radiation increases with increasing tube voltage. Vasconcelos et al. showed that increasing the tube voltage from 70 kVp to 90 kVp in CBCT increased the effective dose more than five-fold (4.08 µSv and 20.91 µSv at low resolution and 18.4 µSv and 93.41 µSv at high resolution, respectively) [11]. Given the significant increase in the effective dose, it should be verified before each exposure whether the benefits of better image quality outweigh the potential risks of higher radiation. The consequences of irradiation might be classified into two groups. Stochastic or linear-dose effects include cancer and hereditary changes in the offspring. The risk increases with an increase in the radiation dose. Deterministic effects involve transient or permanent tissue damage and acute radiation syndrome, which occur when cells are killed by a high dose of radiation. They are observed when doses exceeding 0.5 Gy are received, although this value might be lower for individual organs; therefore, it does not have to be taken into account in diagnostic tests such as CBCT where the absorbed dose is much lower [46].

Conclusions

CBCT is the gold standard in the pre- and postoperative diagnosis as well as treatment of peri-implantitis. Due to the growing interest in the treatment with dental implants, many studies are currently conducted to achieve the lowest possible number of metal artifacts in CBCT. From the literature review, it might be drawn that dental artifacts are a significant limitation in the diagnosis of peri-implant tissues, and it is possible to reduce the incidence of artifacts and improve the image quality by appropriately modifying the exposure parameters. The reduction of artifacts is often associated with a significant increase in radiation; therefore, effort should be taken to minimize the radiation dose in accordance with the ALARA principle. Undoubtedly, there is a need to conduct further studies to improve the CBCT exposure protocol to improve the image quality and increase the diagnostic efficacy in peri-implant pathologies, which would allow for their early diagnosis and treatment.

Additional Information

Disclosures

Conflicts of interest: In compliance with the ICMJE uniform disclosure form, all authors declare the following: **Payment/services info:** All authors have declared that no financial support was received from any organization for the submitted work. **Financial relationships:** All authors have declared that they have no financial relationships at present or within the previous three years with any organizations that might have an interest in the submitted work. **Other relationships:** All authors have declared that there are no other relationships or activities that could appear to have influenced the submitted work.

References

1. Jacobs R, Salmon B, Codari M, Hassan B, Bornstein MM: Cone beam computed tomography in implant dentistry: recommendations for clinical use. BMC Oral Health. 2018, 18:88. 10.1186/s12903-018-0523-5
2. McGuigan MB, Duncan HF, Horner K: An analysis of effective dose optimization and its impact on image quality and diagnostic efficacy relating to dental cone beam computed tomography (CBCT). Swiss Dent J. 2018, 128:297-316.
3. Dreyer H, Grischke J, Tiede C, et al.: Epidemiology and risk factors of peri-implantitis: a systematic review . J Periodontal Res. 2018, 53:657-81. 10.1111/jre.12562
4. Nascimento EH, Fontenele RC, Santaella GM, Freitas DQ: Difference in the artefacts production and the performance of the metal artefact reduction (MAR) tool between the buccal and lingual cortical plates adjacent to zirconium dental implant. Dentomaxillofac Radiol. 2019, 48:20190058. 10.1259/dmfr.20190058
5. Schulze RK, Berndt D, d'Hoedt B: On cone-beam computed tomography artifacts induced by titanium implants. Clin Oral Implants Res. 2010, 21:100-7. 10.1111/j.1600-0501.2009.01817.x
6. Draenert FG, Coppenrath E, Herzog P, Müller S, Mueller-Lisse UG: Beam hardening artefacts occur in dental implant scans with the NewTom cone beam CT but not with the dental 4-row multidetector CT. Dentomaxillofac Radiol. 2007, 36:198-203. 10.1259/dmfr/32579161
7. Schulze R, Heil U, Gross D, Bruellmann DD, Dranischnikow E, Schwanecke U, Schoemer E: Artefacts in CBCT: a review. Dentomaxillofac Radiol. 2011, 40:265-73. 10.1259/dmfr/30642039
8. Różyło-Kalinowska I, Miechowicz S, Sarna-Boś K, Borowicz J, Kalinowski P: Analysis of vector models in quantification of artifacts produced by standard prosthetic inlays in cone-beam computed tomography (CBCT)--a preliminary study. Postepy Hig Med Dosw (Online). 2014, 68:1343-6. 10.5604/17322693.1129139
9. Barrett JF, Keat N: Artifacts in CT: recognition and avoidance. Radiographics. 2004, 24:1679-91. 10.1148/rg.246045065
10. Spin-Neto R, Gotfredsen E, Wenzel A: Impact of voxel size variation on CBCT-based diagnostic outcome in dentistry: a systematic review. J Digit Imaging. 2013, 26:813-20. 10.1007/s10278-012-9562-7
11. Vasconcelos TV, Bechara BB, McMahan CA, Freitas DQ, Noujeim M: Evaluation of artifacts generated by zirconium implants in cone-beam computed tomography images. Oral Surg Oral Med Oral Pathol Oral Radiol. 2017, 123:265-72. 10.1016/j.oooo.2016.10.021
12. Sun X, Zhao Q, Sun P, Yao Z, Wang R: Metal artifact reduction using mono-energy images combined with metal artifact reduction software in spectral computed tomography: a study on phantoms. Quant Imaging Med Surg. 2020, 10:1515-25. 10.21037/qims-19-936
13. Chindasombatjaroen J, Kakimoto N, Murakami S, Maeda Y, Furukawa S: Quantitative analysis of metallic artifacts caused by dental metals: comparison of cone-beam and multi-detector row CT scanners. Oral Radiology. 2011, 27:114-120. 10.1007/s11282-011-0071-z
14. Pauwels R, Araki K, Siewerdsen JH, Thongvigitmanee SS: Technical aspects of dental CBCT: state of the art . Dentomaxillofac Radiol. 2015, 44:20140224. 10.1259/dmfr.20140224
15. Boas F, Fleischmann D: CT artifacts: causes and reduction techniques . Imaging Med. 2012, 4:229-40. 10.2217/iim.12.13
16. Panjnoush M, Kheirandish Y, Kashani PM, Fakhar HB, Younesi F, Mallahi M: Effect of exposure parameters on metal artifacts in cone beam computed tomography. J Dent (Tehran). 2016, 13:143-50.
17. Shokri A, Jamalpour MR, Khavid A, Mohseni Z, Sadeghi M: Effect of exposure parameters of cone beam

computed tomography on metal artifact reduction around the dental implants in various bone densities. BMC Med Imaging. 2019, 19:34. 10.1186/s12880-019-0334-4
18. Pauwels R, Stamatakis H, Bosmans H, Bogaerts R, Jacobs R, Horner K, Tsiklakis K: Quantification of metal artifacts on cone beam computed tomography images. Clin Oral Implants Res. 2013, 24:94-9. 10.1111/j.1600-0501.2011.02382.x
19. Fontenele RC, Farias Gomes A, Nejaim Y, Freitas DQ: Do the tube current and metal artifact reduction influence the diagnosis of vertical root fracture in a tooth positioned in the vicinity of a zirconium implant? A CBCT study. Clin Oral Investig. 2021, 25:2229-35. 10.1007/s00784-020-03538-4
20. Pauwels R, Zhang G, Theodorakou C, et al.: Effective radiation dose and eye lens dose in dental cone beam CT: effect of field of view and angle of rotation. Br J Radiol. 2014, 87:20130654. 10.1259/bjr.20130654
21. Costa ED, Queiroz PM, Santaella GM, Capelozza AL, Ambrosano GM, Freitas DQ: Influence of scan mode (partial/full rotations) and FOV size in the formation of artefacts in cone beam CT. Dentomaxillofac Radiol. 2019, 48:20180340. 10.1259/dmfr.20180340
22. Bechara B, McMahan CA, Geha H, Noujeim M: Evaluation of a cone beam CT artefact reduction algorithm . Dentomaxillofac Radiol. 2012, 41:422-8. 10.1259/dmfr/43691321
23. Parsa A, Ibrahim N, Hassan B, Motroni A, van der Stelt P, Wismeijer D: Influence of cone beam CT scanning parameters on grey value measurements at an implant site. Dentomaxillofac Radiol. 2013, 42:79884780. 10.1259/dmfr/79884780
24. Nikbin A, Dalili Kajan Z, Taramsari M, Khosravifard N: Effect of object position in the field of view and application of a metal artifact reduction algorithm on the detection of vertical root fractures on cone-beam computed tomography scans: an in vitro study. Imaging Sci Dent. 2018, 48:245-54. 10.5624/isd.2018.48.4.245
25. Nagarajappa AK, Dwivedi N, Tiwari R: Artifacts: the downturn of CBCT image . J Int Soc Prev Community Dent. 2015, 5:440-5. 10.4103/2231-0762.170523
26. Bechara B, McMahan CA, Moore WS, Noujeim M, Geha H, Teixeira FB: Contrast-to-noise ratio difference in small field of view cone beam computed tomography machines. J Oral Sci. 2012, 54:227-32. 10.2334/josnusd.54.227
27. Rawson JV: CBCT: wide range of clinical applications and wide range of doses . Ann ICRP. 2015, 44:7-8. 10.1177/0146645315575485
28. Brüllmann D, Schulze RK: Spatial resolution in CBCT machines for dental/maxillofacial applications-what do we know today?. Dentomaxillofac Radiol. 2015, 44:20140204. 10.1259/dmfr.20140204
29. Lue KH, Lin HH, Kao CH, Hsieh HJ, Liu SH, Chuang KS: A simple algorithm for subregional striatal uptake analysis with partial volume correction in dopaminergic PET imaging. Ann Nucl Med. 2014, 28:33-41. 10.1007/s12149-013-0778-5
30. Kursun-Cakmak EŞ, Demirturk Kocasarac H, Bayrak S, Ustaoğlu G, Noujeim M: Estimation of contrast-to-noise ratio in CT and CBCT images with varying scan settings in presence of different implant materials. Dentomaxillofac Radiol. 2019, 48:20190139. 10.1259/dmfr.20190139
31. Vasconcelos TV, Leandro Nascimento EH, Bechara BB, Freitas DQ, Noujeim M: Influence of cone beam computed tomography settings on implant artifact production: zirconia and titanium. Int J Oral Maxillofac Implants. 2019, 34:1114-20. 10.11607/jomi.7129
32. Schwindling FS, Hilgenfeld T, Weber D, Kosinski MA, Rammelsberg P, Tasaka A: In vitro diagnostic accuracy of low-dose CBCT for evaluation of peri-implant bone lesions. Clin Oral Implants Res. 2019, 30:1200-8. 10.1111/clr.13533
33. Fontenele RC, Nascimento EH, Santaella GM, Freitas DQ: Does the metal artifact reduction algorithm activation mode influence the magnitude of artifacts in CBCT images?. Imaging Sci Dent. 2020, 50:23-30. 10.5624/isd.2020.50.1.23
34. de Faria Vasconcelos K, Queiroz PM, Codari M, Nicolielo LFP, Freitas DQ, Jacobs R, Haiter-Neto F: A quantitative analysis of metal artifact reduction algorithm performance in volume correction with 3 CBCT devices. Oral Surg Oral Med Oral Pathol Oral Radiol. 2020, 130:328-35. 10.1016/j.oooo.2020.03.049
35. Candemil AP, Salmon B, Freitas DQ, Ambrosano GM, Haiter-Neto F, Oliveira ML: Are metal artefact reduction algorithms effective to correct cone beam CT artefacts arising from the exomass?. Dentomaxillofac Radiol. 2019, 48:20180290. 10.1259/dmfr.20180290
36. Vasconcelos KF, Codari M, Queiroz PM, et al.: The performance of metal artifact reduction algorithms in cone beam computed tomography images considering the effects of materials, metal positions, and fields of view. Oral Surg Oral Med Oral Pathol Oral Radiol. 2019, 127:71-6. 10.1016/j.oooo.2018.09.004
37. Queiroz PM, Santaella GM, Groppo FC, Freitas DQ: Metal artifact production and reduction in CBCT with different numbers of basis images. Imaging Sci Dent. 2018, 48:41-4. 10.5624/isd.2018.48.1.41
38. Bechara B, McMahan CA, Nasseh I, et al.: Number of basis images effect on detection of root fractures in endodontically treated teeth using a cone beam computed tomography machine: an in vitro study. Oral Surg Oral Med Oral Pathol Oral Radiol. 2013, 115:676-81. 10.1016/j.oooo.2013.01.026
39. Kamburoglu K, Kolsuz E, Murat S, Eren H, Yüksel S, Paksoy CS: Assessment of buccal marginal alveolar peri-implant and periodontal defects using a cone beam CT system with and without the application of metal artefact reduction mode. Dentomaxillofac Radiol. 2013, 42:20130176. 10.1259/dmfr.20130176
40. de-Azevedo-Vaz SL, Peyneau PD, Ramirez-Sotelo LR, Vasconcelos Kde F, Campos PS, Haiter-Neto F: Efficacy of a cone beam computed tomography metal artifact reduction algorithm for the detection of peri-implant fenestrations and dehiscences. Oral Surg Oral Med Oral Pathol Oral Radiol. 2016, 121:550-6. 10.1016/j.oooo.2016.01.013
41. Bechara B, Alex McMahan C, Moore WS, Noujeim M, Teixeira FB, Geha H: Cone beam CT scans with and without artefact reduction in root fracture detection of endodontically treated teeth. Dentomaxillofac Radiol. 2013, 42:20120245. 10.1259/dmfr.20120245
42. Katsumata A, Hirukawa A, Okumura S, Naitoh M, Fujishita M, Ariji E, Langlais RP: Relationship between density variability and imaging volume size in cone-beam computerized tomographic scanning of the maxillofacial region: an in vitro study. Oral Surg Oral Med Oral Pathol Oral Radiol Endod. 2009, 107:420-5. 10.1016/j.tripleo.2008.05.049

43. Bechara BB, Moore WS, McMahan CA, Noujeim M: Metal artefact reduction with cone beam CT: an in vitro study. Dentomaxillofac Radiol. 2012, 41:248-53. 10.1259/dmfr/80899839
44. Keith H: Radiation protection 172. Cone beam CT for dental and maxillofacial radiology: evidence-based guidelines. European Commission, Luxembourg; 2012.
45. Atci IB, Yilmaz H, Antar V, et al.: What do we know about ALARA? Is our knowledge sufficient about radiation safety?. J Neurosurg Sci. 2017, 61:597-602. 10.23736/S0390-5616.16.03418-4
46. De Felice F, Di Carlo G, Saccucci M, Tombolini V, Polimeni A: Dental cone beam computed tomography in children: clinical effectiveness and cancer risk due to radiation exposure. Oncology. 2019, 96:173-8. 10.1159/000497059

IX. Oświadczenia współautorów publikacji

Warszawa, 7 września 2022r.
(miejscowość, data)

Paweł Sawicki
(imię i nazwisko)

OŚWIADCZENIE

Jako współautor pracy pt. „Influence of Exposure Parameters and Implant Position in Peri-Implant Bone Assessment in CBCT Images: An In Vitro Study." oświadczam, iż mój własny wkład merytoryczny w przygotowanie, przeprowadzenie i opracowanie badań oraz przedstawienie pracy w formie publikacji stanowi:

- Opracowanie koncepcji i metodologii
- Przygotowanie materiału do badań
- Wykonanie badań
- Interpretacja wyników
- Przygotowanie manuskryptu
- Ostateczna ocena artykułu przed oddaniem do recenzji

Mój udział procentowy w przygotowaniu publikacji określam jako 80 %.

Paweł Sawicki

....
(podpis oświadczającego)

Warszawa, 7 września 2022r.
(miejscowość, data)

Piotr Regulski
(imię i nazwisko)

OŚWIADCZENIE

Jako współautor pracy pt. „Influence of Exposure Parameters and Implant Position in Peri-Implant Bone Assessment in CBCT Images: An In Vitro Study." oświadczam, iż mój własny wkład merytoryczny w przygotowanie, przeprowadzenie i opracowanie badań oraz przedstawienie pracy w formie publikacji stanowi:

- Opracowanie koncepcji i metodologii
- Współpraca przy powstawaniu manuskryptu
- Ostateczna ocena artykułu przed oddaniem do recenzji

Mój udział procentowy w przygotowaniu publikacji określam jako 10 %.
Wkład Pawła Sawickiego w powstawanie publikacji określam jako 80 %,
(imię i nazwisko kandydata do stopnia)

obejmował on:

- Opracowanie koncepcji i metodologii
- Przygotowanie materiału do badań
- Wykonanie badań
- Interpretacja wyników
- Przygotowanie manuskryptu
- Ostateczna ocena artykułu przed oddaniem do recenzji

(merytoryczny opis wkładu kandydata do stopnia w powstanie publikacji)

Jednocześnie wyrażam zgodę na wykorzystanie w/w pracy jako część rozprawy doktorskiej lek. dent. Pawła Sawickiego
(imię i nazwisko kandydata do stopnia)

Piotr Regulski
....
(podpis oświadczającego)

Warszawa, 7 września 2022r.
(miejscowość, data)

Artur Winiarski
(imię i nazwisko)

OŚWIADCZENIE

Jako współautor pracy pt. „Influence of Exposure Parameters and Implant Position in Peri-Implant Bone Assessment in CBCT Images: An In Vitro Study." oświadczam, iż mój własny wkład merytoryczny w przygotowanie, przeprowadzenie i opracowanie badań oraz przedstawienie pracy w formie publikacji stanowi:

- Przygotowanie części materiału do dalszych badań

Mój udział procentowy w przygotowaniu publikacji określam jako 8 %.
Wkład Pawła Sawickiego w powstawanie publikacji określam jako 80 %,
(imię i nazwisko kandydata do stopnia)

obejmował on:

- Opracowanie koncepcji i metodologii
- Przygotowanie materiału do badań
- Wykonanie badań
- Interpretacja wyników
- Przygotowanie manuskryptu
- Ostateczna ocena artykułu przed oddaniem do recenzji

(merytoryczny opis wkładu kandydata do stopnia w powstanie publikacji)*

Jednocześnie wyrażam zgodę na wykorzystanie w/w pracy jako część rozprawy doktorskiej lek. dent. Pawła Sawickiego
(imię i nazwisko kandydata do stopnia)

....
(podpis oświadczającego)

*w szczególności udziału w przygotowaniu koncepcji, metodyki, wykonaniu badań, interpretacji wyników

Warszawa, 7 września 2022r.
(miejscowość, data)

Paweł Zawadzki
(imię i nazwisko)

OŚWIADCZENIE

Jako współautor pracy pt. „Influence of Exposure Parameters and Implant Position in Peri-Implant Bone Assessment in CBCT Images: An In Vitro Study." oświadczam, iż mój własny wkład merytoryczny w przygotowanie, przeprowadzenie i opracowanie badań oraz przedstawienie pracy w formie publikacji stanowi:

- Ostateczna ocena artykułu przed oddaniem do recenzji

Mój udział procentowy w przygotowaniu publikacji określam jako 2 %.
Wkład Pawła Sawickiego w powstawanie publikacji określam jako 80 %,
(imię i nazwisko kandydata do stopnia)

obejmował on:

- Opracowanie koncepcji i metodologii
- Przygotowanie materiału do badań
- Wykonanie badań
- Interpretacja wyników
- Przygotowanie manuskryptu
- Ostateczna ocena artykułu przed oddaniem do recenzji

(merytoryczny opis wkładu kandydata do stopnia w powstanie publikacji)

Jednocześnie wyrażam zgodę na wykorzystanie w/w pracy jako część rozprawy doktorskiej lek. dent. Pawła Sawickiego
(imię i nazwisko kandydata do stopnia)

Paweł Zawadzki
....
(podpis oświadczającego)

Warszawa, 7 września 2022r.
(miejscowość, data)

Paweł Sawicki
(imię i nazwisko)

OŚWIADCZENIE

Jako współautor pracy pt. „The Impact of Cone-Beam Computed Tomography Exposure Parameters on Peri-Implant Artifacts: A Literature Review" oświadczam, iż mój własny wkład merytoryczny w przygotowanie, przeprowadzenie i opracowanie badań oraz przedstawienie pracy w formie publikacji stanowi:

- Opracowanie koncepcji i metodologii
- Przygotowanie przeglądu piśmiennictwa
- Interpretacja wyników
- Przygotowanie manuskryptu
- Ostateczna ocena artykułu przed oddaniem do recenzji

Mój udział procentowy w przygotowaniu publikacji określam jako 90 %.

Paweł Sawicki
....
(podpis oświadczającego)

Warszawa, 7 września 2022r.
(miejscowość, data)

Piotr Regulski
(imię i nazwisko)

OŚWIADCZENIE

Jako współautor pracy pt. „The Impact of Cone-Beam Computed Tomography Exposure Parameters on Peri-Implant Artifacts: A Literature Review" oświadczam, iż mój własny wkład merytoryczny w przygotowanie, przeprowadzenie i opracowanie badań oraz przedstawienie pracy w formie publikacji stanowi:

- Udział w tworzeniu projektu
- Ostateczna ocena artykułu przed oddaniem do recenzji

Mój udział procentowy w przygotowaniu publikacji określam jako 8 %.
Wkład Pawła Sawickiego w powstawanie publikacji określam jako 90 %,
(imię i nazwisko kandydata do stopnia)

obejmował on:

- Opracowanie koncepcji i metodologii
- Przygotowanie przeglądu piśmiennictwa
- Interpretacja wyników
- Przygotowanie manuskryptu
- Ostateczna ocena artykułu przed oddaniem do recenzji

(merytoryczny opis wkladu kandydata do stopnia w powstanie publikacji)

Jednocześnie wyrażam zgodę na wykorzystanie w/w pracy jako część rozprawy doktorskiej lek. dent. Pawła Sawickiego
(imię i nazwisko kandydata do stopnia)

Piotr Regulski
....
(podpis oświadczającego)

Warszawa, 7 września 2022r.
(miejscowość, data)

Paweł Zawadzki
(imię i nazwisko)

OŚWIADCZENIE

Jako współautor pracy pt. „The Impact of Cone-Beam Computed Tomography Exposure Parameters on Peri-Implant Artifacts: A Literature Review" oświadczam, iż mój własny wkład merytoryczny w przygotowanie, przeprowadzenie i opracowanie badań oraz przedstawienie pracy w formie publikacji stanowi:

- Ostateczna ocena artykułu przed oddaniem do recenzji

Mój udział procentowy w przygotowaniu publikacji określam jako 2 %.
Wkład Pawła Sawickiego w powstawanie publikacji określam jako 90 %,
(imię i nazwisko kandydata do stopnia)

obejmował on:

- Opracowanie koncepcji i metodologii
- Przygotowanie przeglądu piśmiennictwa
- Interpretacja wyników
- Przygotowanie manuskryptu
- Ostateczna ocena artykułu przed oddaniem do recenzji

(merytoryczny opis wkładu kandydata do stopnia w powstanie publikacji)

Jednocześnie wyrażam zgodę na wykorzystanie w/w pracy jako część rozprawy doktorskiej lek. dent. Pawła Sawickiego
(imię i nazwisko kandydata do stopnia)

....
(podpis oświadczającego)